

# Supplements to Examining NHD vs QHD in the GCM THOR with non-grey radiative transfer for the hot Jupiter regime

Pascal A. Noti,<sup>1,2</sup>  Elspeth K. H. Lee,<sup>1</sup>  Russell Deitrick<sup>3</sup>  and Mark Hammond<sup>4</sup> 

<sup>1</sup>*Center for Space and Habitability, Universität Bern, Gesellschaftsstrasse 6, CH-3012 Bern, Switzerland*

<sup>2</sup>*Physikalisches Institut, Universität Bern, Sidlerstrasse 5, CH-3012 Bern, Switzerland*

<sup>3</sup>*School of Earth and Ocean Sciences, University of Victoria, Victoria, British Columbia, Canada*

<sup>4</sup>*Atmospheric, Oceanic and Planetary Physics, University of Oxford, Oxford, United Kingdom*

Accepted XXX. Received YYY; in original form ZZZ

## 1 GCM SIMULATIONS

### 1.1 Altering Rotation Rate at low gravity

### 1.2 Altering Gravity

### 1.3 Altering Irradiance Temperature at low gravity

### 1.4 Altering Rotation Rate at high gravity

### 1.5 Altering Irradiance Temperature at high gravity

This paper has been typeset from a T<sub>E</sub>X/L<sup>A</sup>T<sub>E</sub>X file prepared by the author.

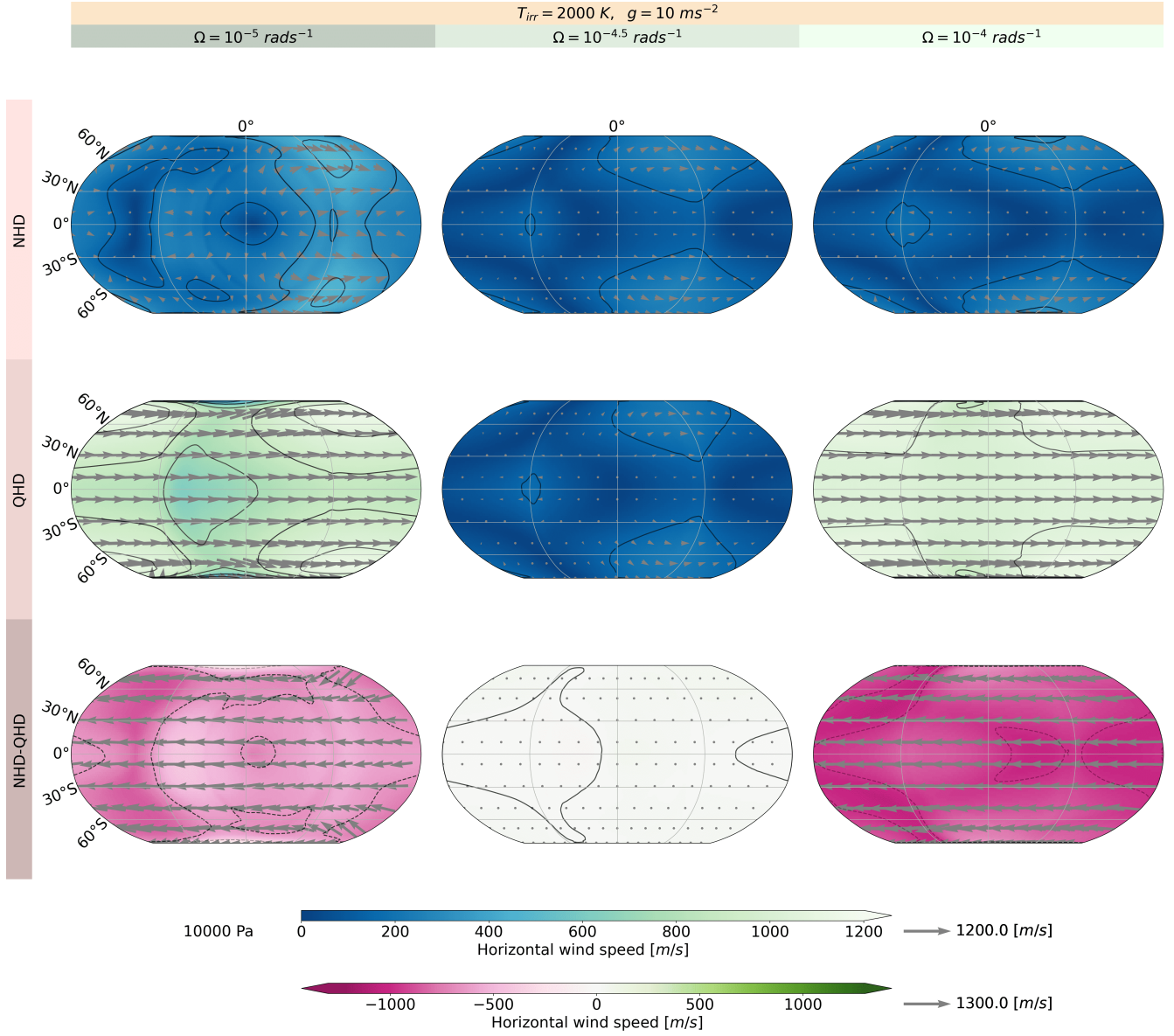


**Figure 1.** Horizontal wind speed at 10'000 Pa for the NHD and QHD equation sets with  $g = 10 \text{ ms}^{-2}$ ,  $T_{irr} = 2'000 \text{ K}$  and with altering  $\Omega$ .



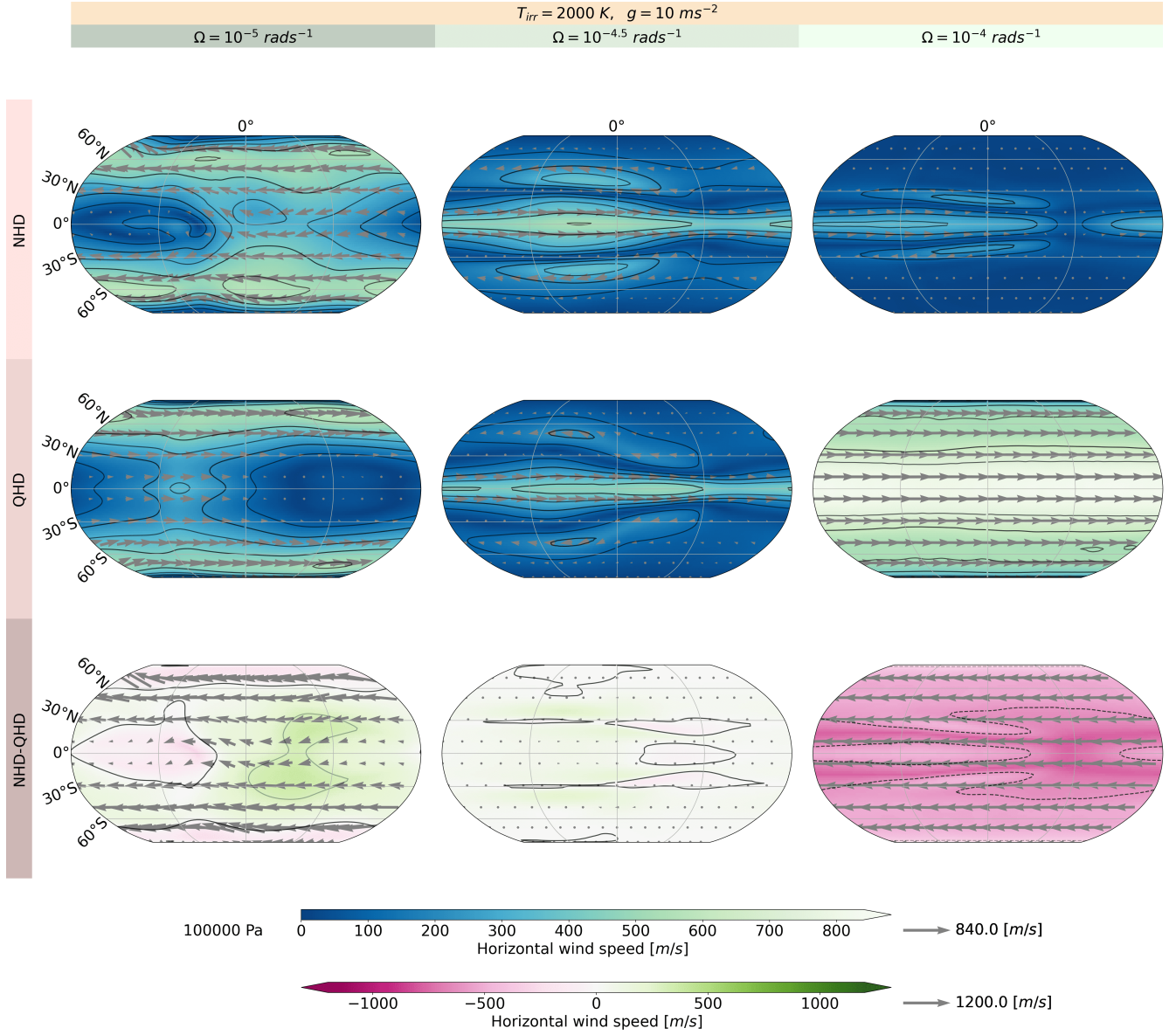


**Figure 2.** Horizontal wind speed at 100'000 Pa for the NHD and QHD equation sets with  $g = 10 \text{ ms}^{-2}$ ,  $T_{irr} = 2'000 \text{ K}$  and with altering  $\Omega$ .

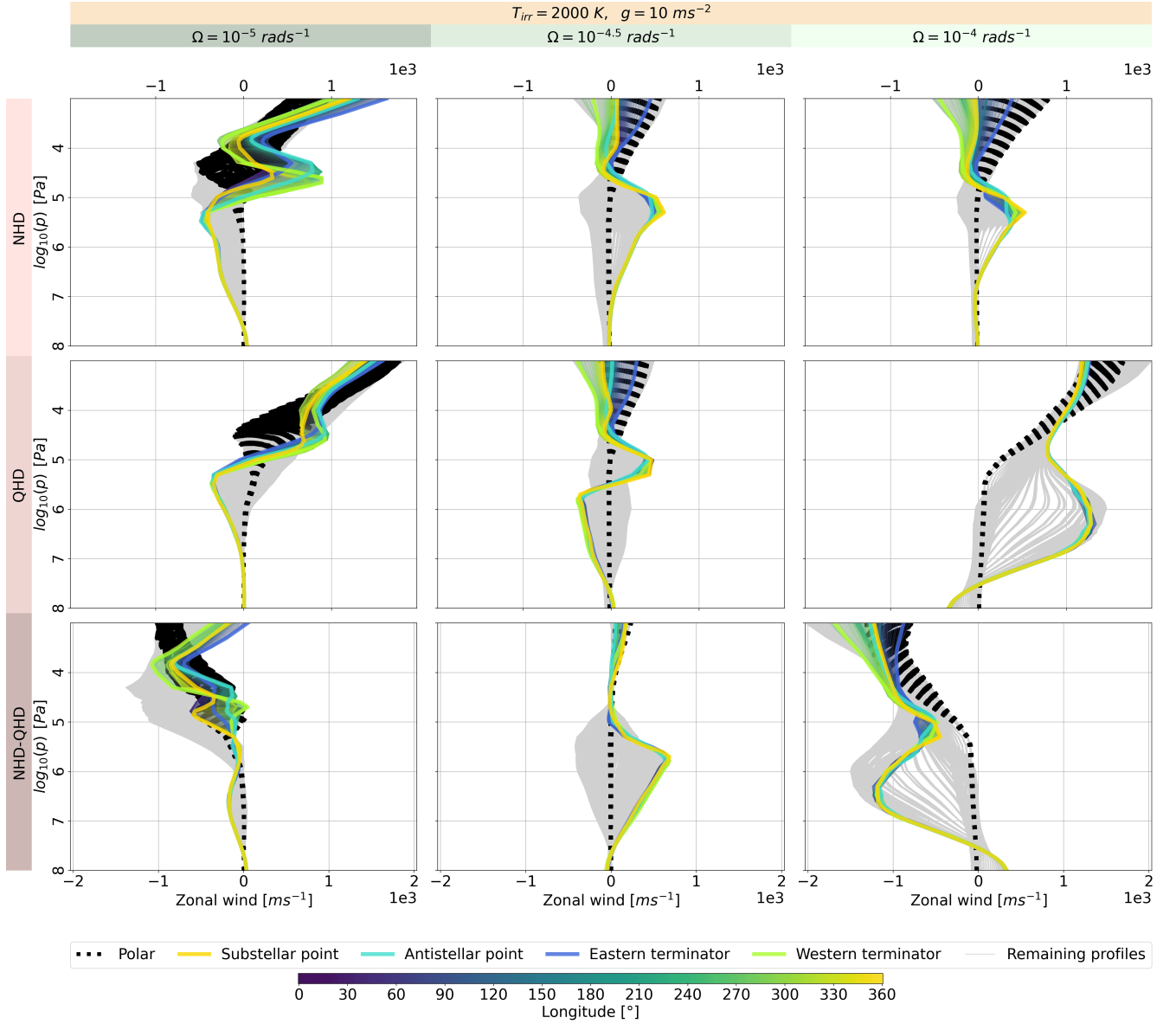


**Figure 3.** Zonal wind speed at each grid point for the NHD and QHD equation sets with  $g = 10 \text{ ms}^{-2}$ ,  $T_{irr} = 2'000 \text{ K}$  and with altering  $\Omega$ . The coloured lines indicate momenta profiles along the equator and its coordinates by the colourbar. The dotted black thin line shows momenta profiles at the latitudes  $87^\circ\text{N}$  and  $87^\circ\text{S}$ . The bold coloured lines represent momenta profiles at the western, eastern terminators, sub- and antistellar point. The grey lines represent all the other momenta profiles.

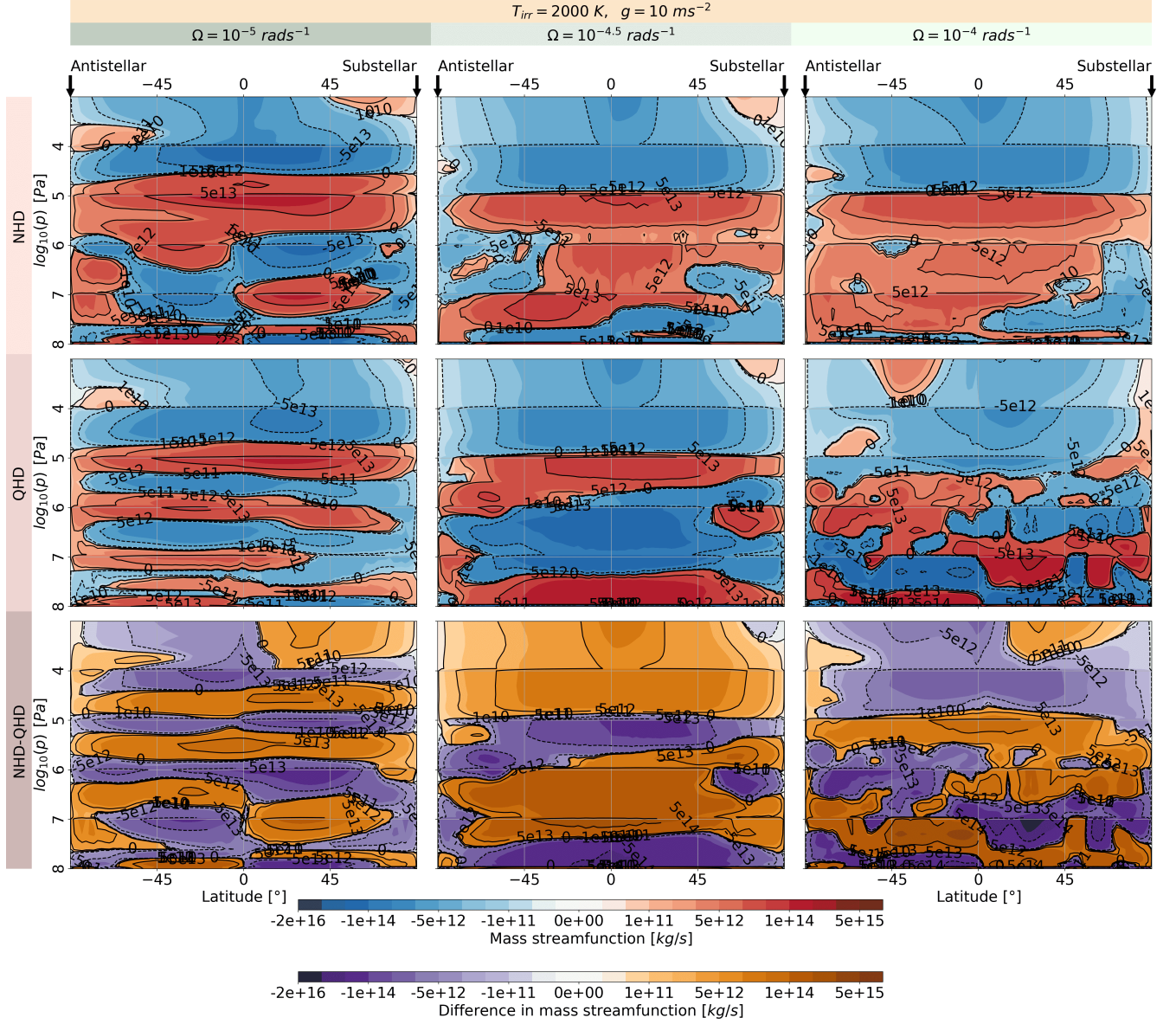


**Figure 4.** Overturning circulation depicted by the streamfunction  $\Psi'$  for the NHD and QHD equation sets with  $g = 10 \text{ ms}^{-2}$ ,  $T_{\text{irr}} = 2'000 \text{ K}$  and with altering  $\Omega$ .

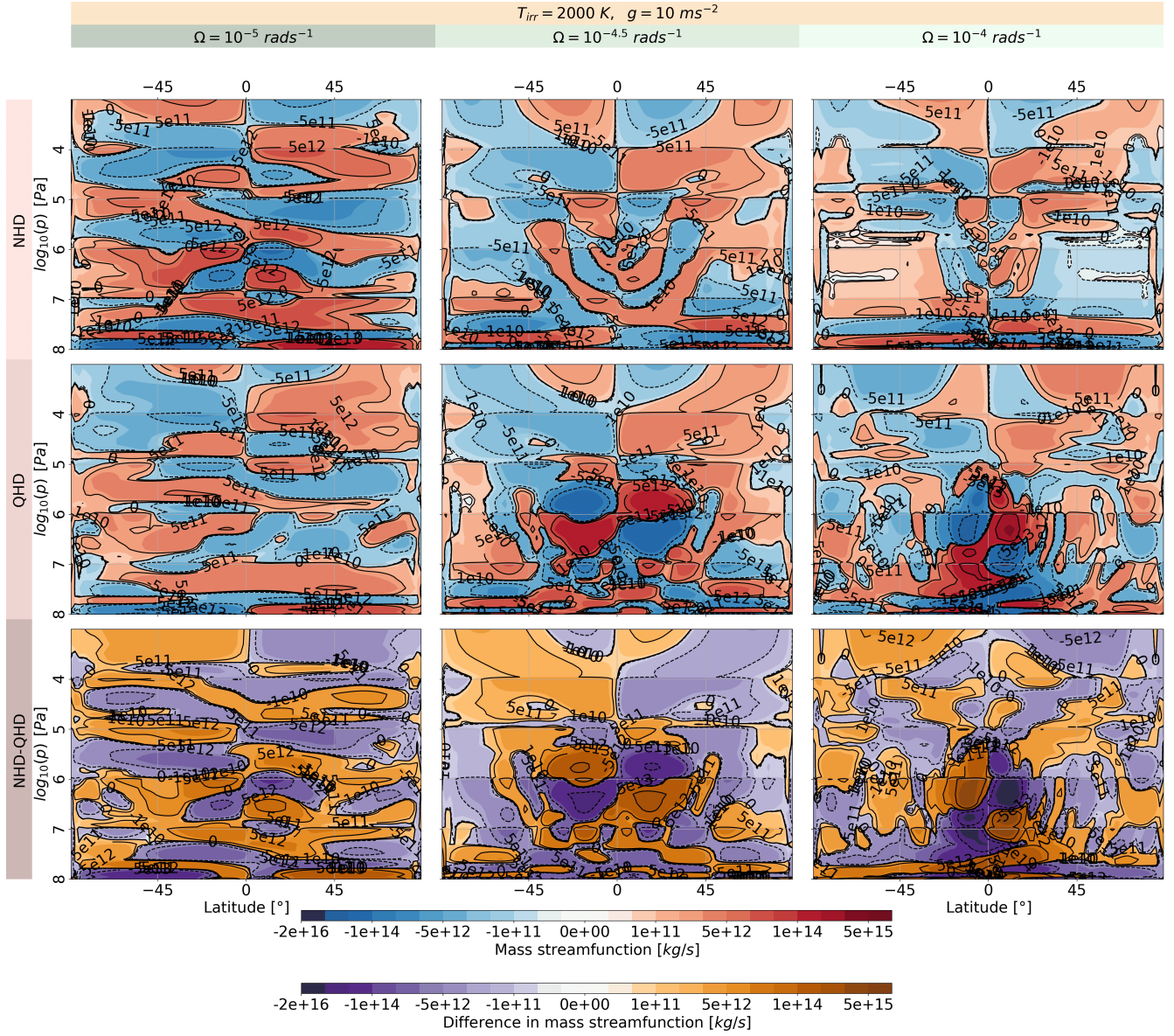


**Figure 5.** Overturning circulation depicted by the streamfunction  $\Psi$  for the NHD and QHD equation sets with  $g = 10 \text{ ms}^{-2}$ ,  $T_{\text{irr}} = 2'000 \text{ K}$  and with altering  $\Omega$ .



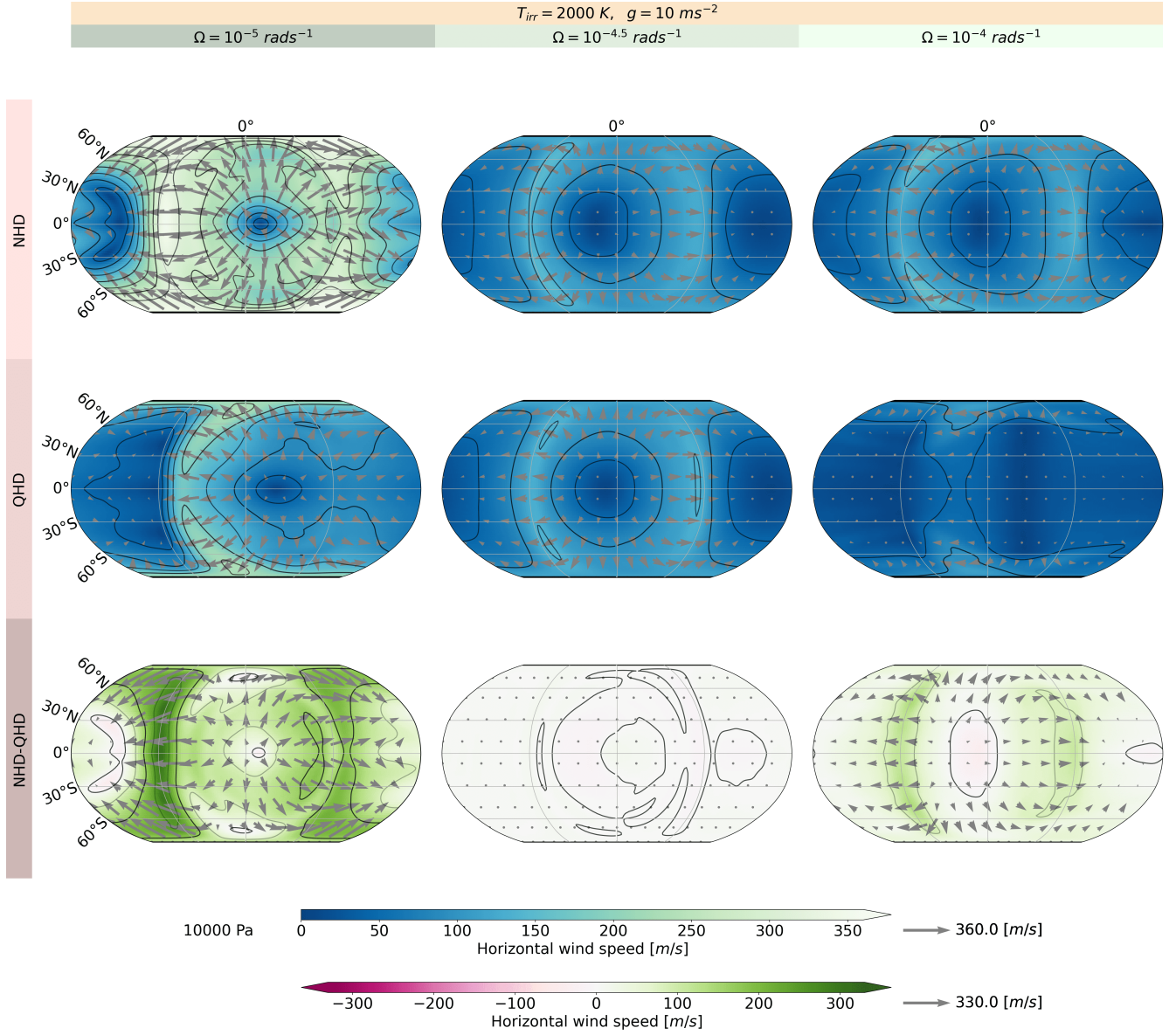


**Figure 6.** Divergent component of the Helmholtz decomposition at 10'000 Pa for the NHD and QHD equation sets with  $g = 10 \text{ ms}^{-2}$ ,  $T_{irr} = 2'000 \text{ K}$  and with altering  $\Omega$ .

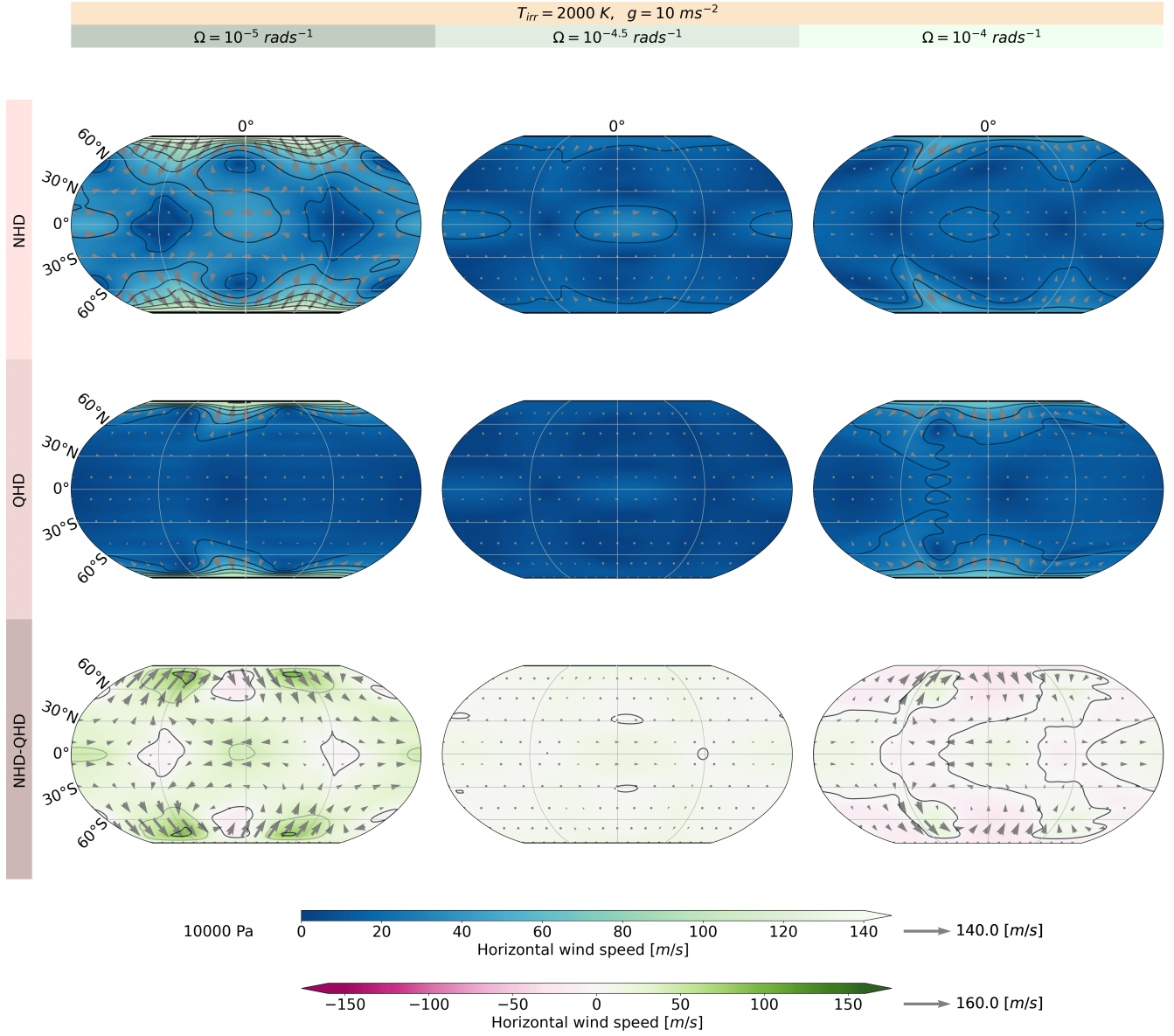


**Figure 7.** Rotational eddy component of the Helmholtz decomposition at  $10'000 \text{ Pa}$  for the NHD and QHD equation sets with  $g = 10 \text{ ms}^{-2}$ ,  $T_{irr} = 2'000 \text{ K}$  and with altering  $\Omega$ .

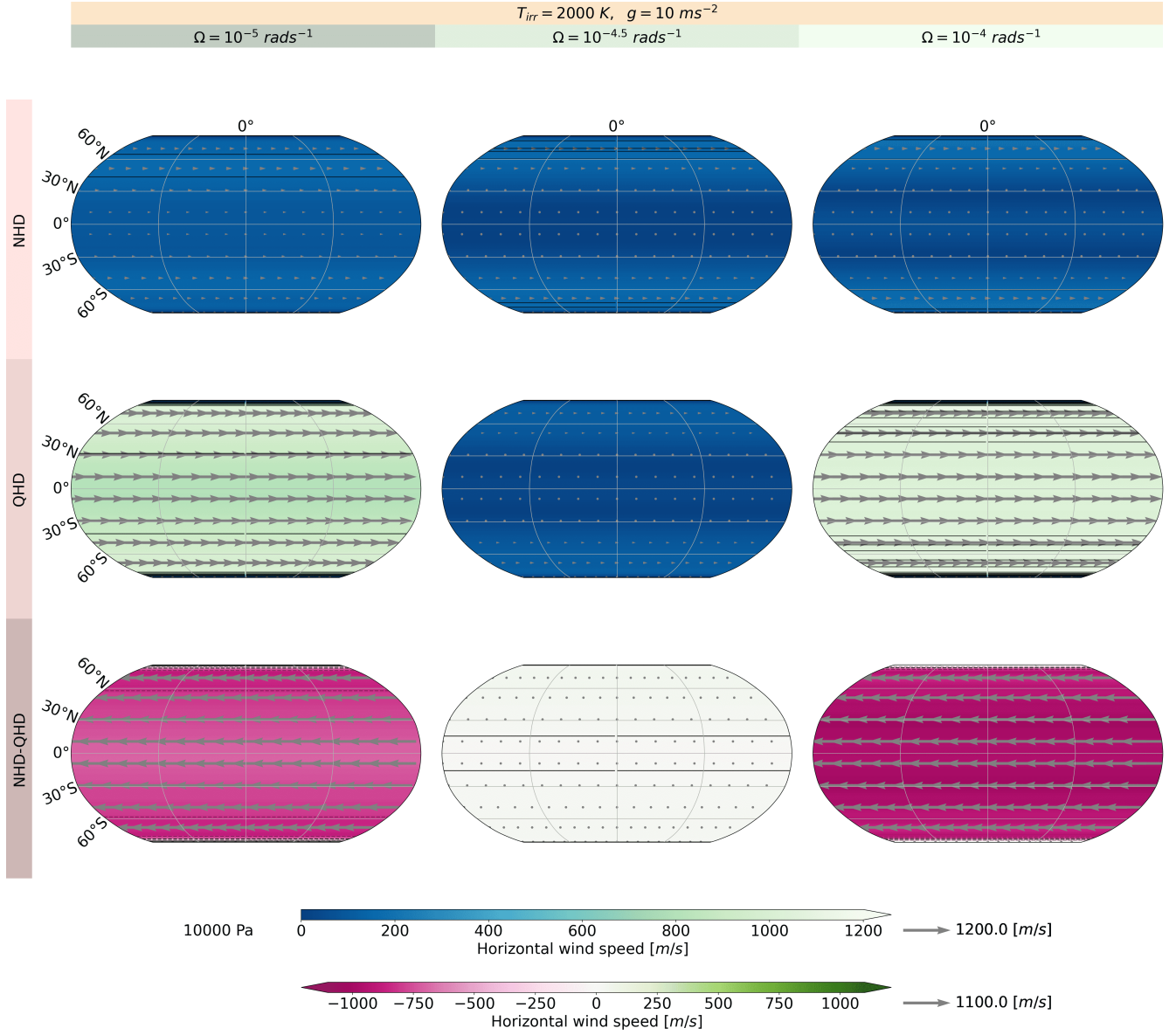


**Figure 8.** Rotational jet component of the Helmholtz decomposition at  $10'000 \text{ Pa}$  for the NHD and QHD equation sets with  $g = 10 \text{ ms}^{-2}$ ,  $T_{irr} = 2'000 \text{ K}$  and with altering  $\Omega$ .



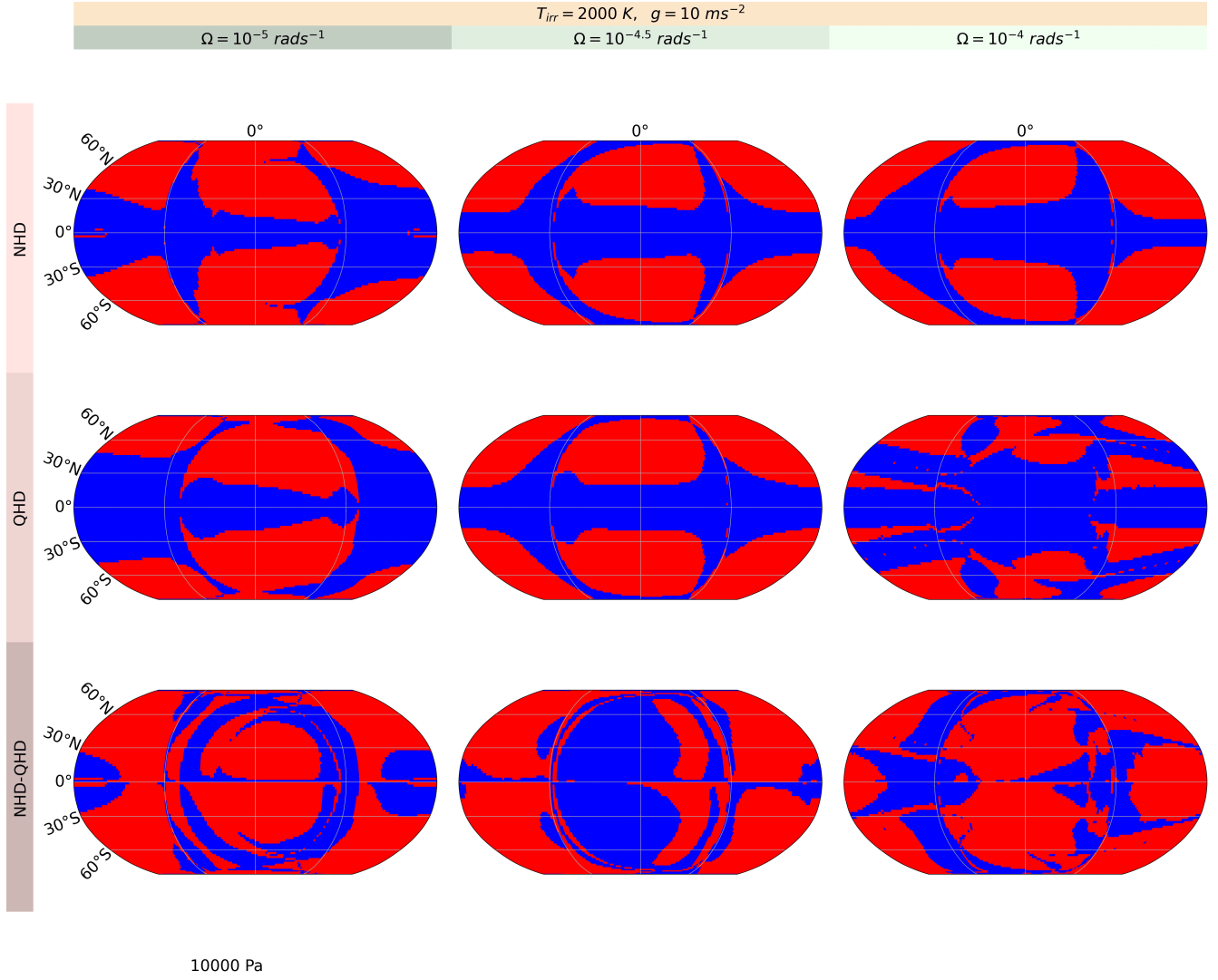


**Figure 9.** Sign of  $\frac{v_{tan}(\Phi)}{10w} - 1$  at 10'000 Pa for the NHD and QHD equation sets with  $g = 10 \text{ ms}^{-2}$ ,  $T_{irr} = 2'000 \text{ K}$  and with altering  $\Omega$ . Dark blue and bright blue regions show negative and positive values

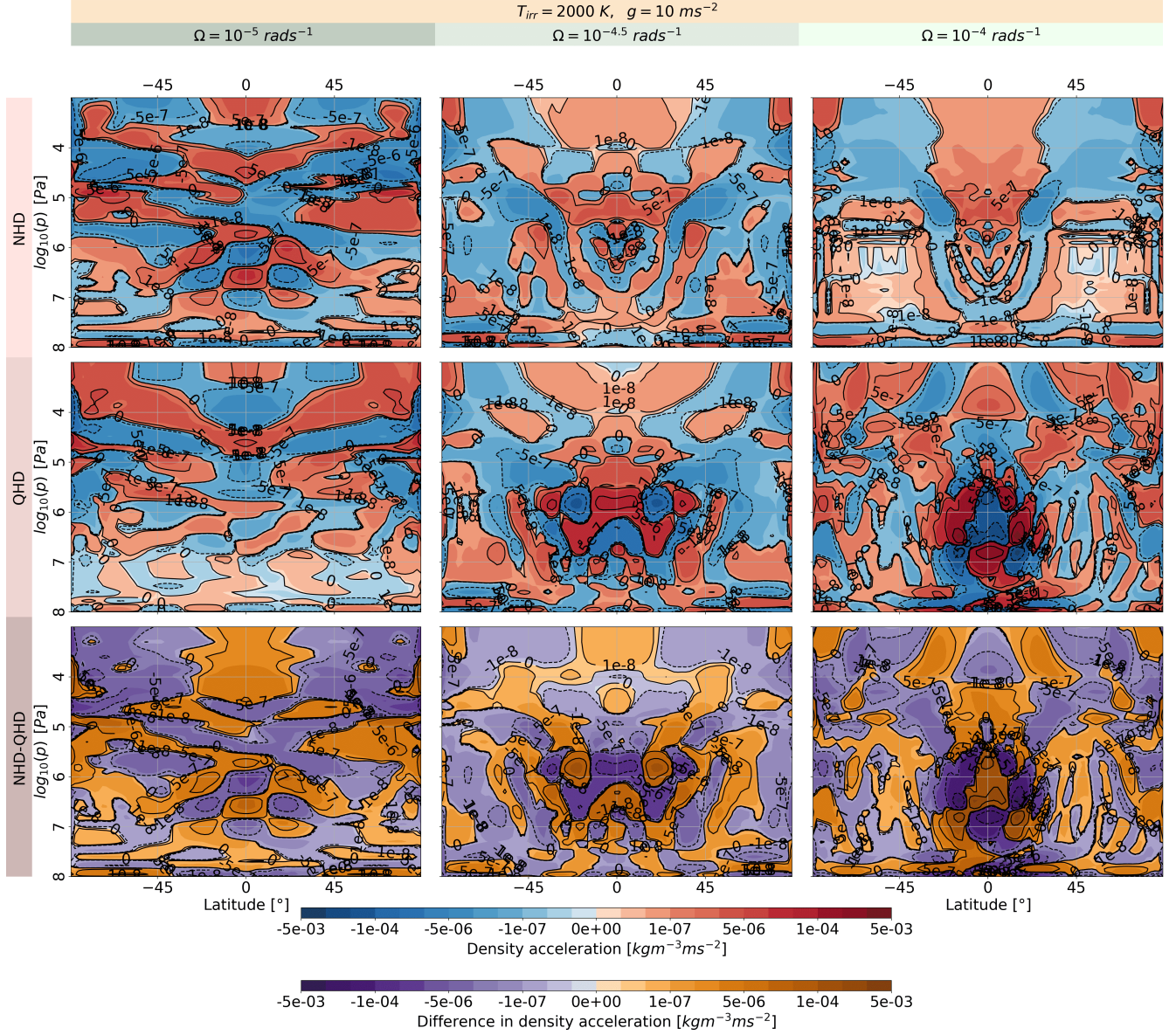


**Figure 10.** Horizontal acceleration for the NHD and QHD equation sets with  $g = 10 \text{ ms}^{-2}$ ,  $T_{\text{irr}} = 2'000 \text{ K}$  and with altering  $\Omega$ .

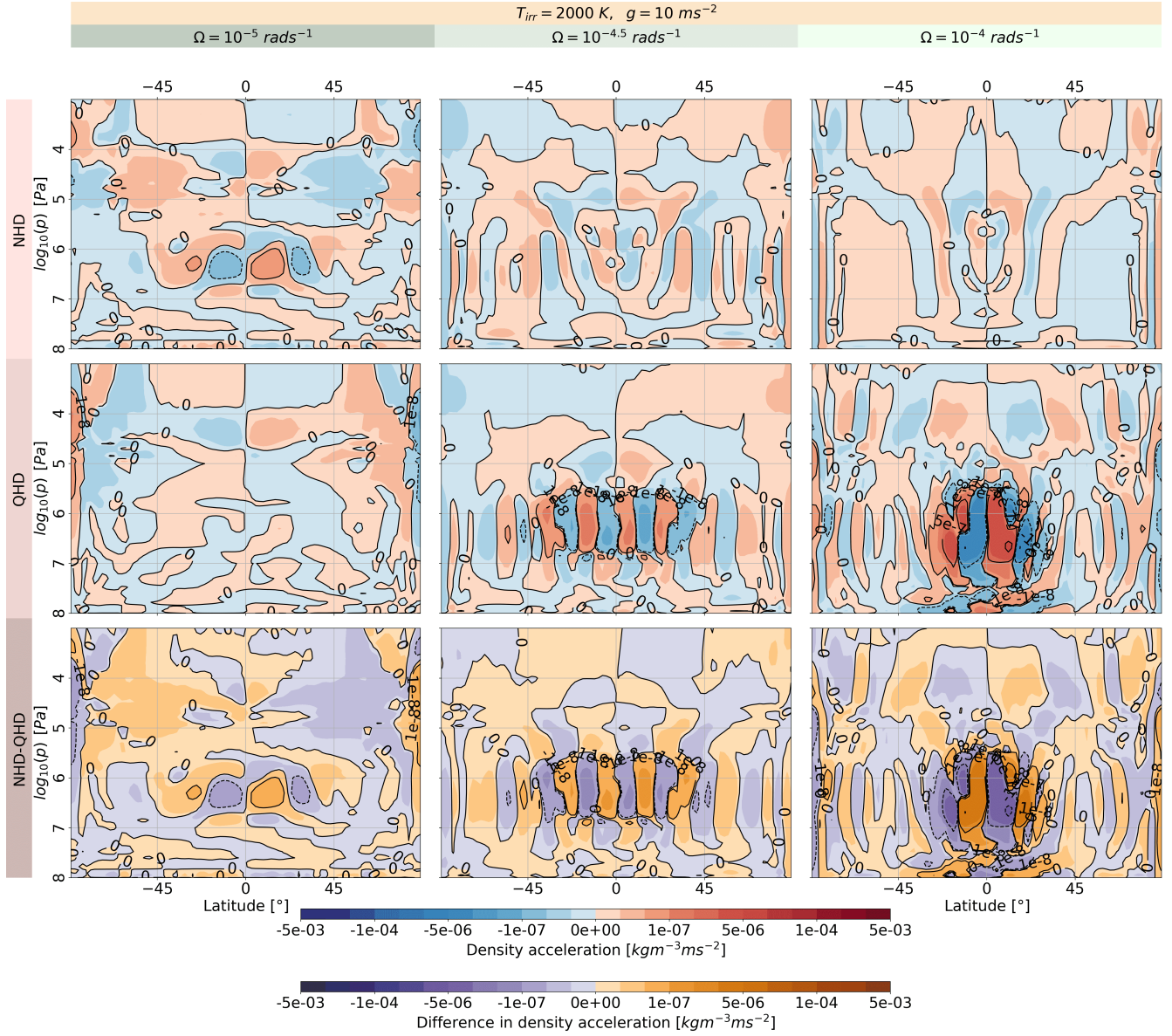


**Figure 11.** Vertical acceleration for the NHD and QHD equation sets with  $g = 10 \text{ ms}^{-2}$ ,  $T_{irr} = 2'000 \text{ K}$  and with altering  $\Omega$ .

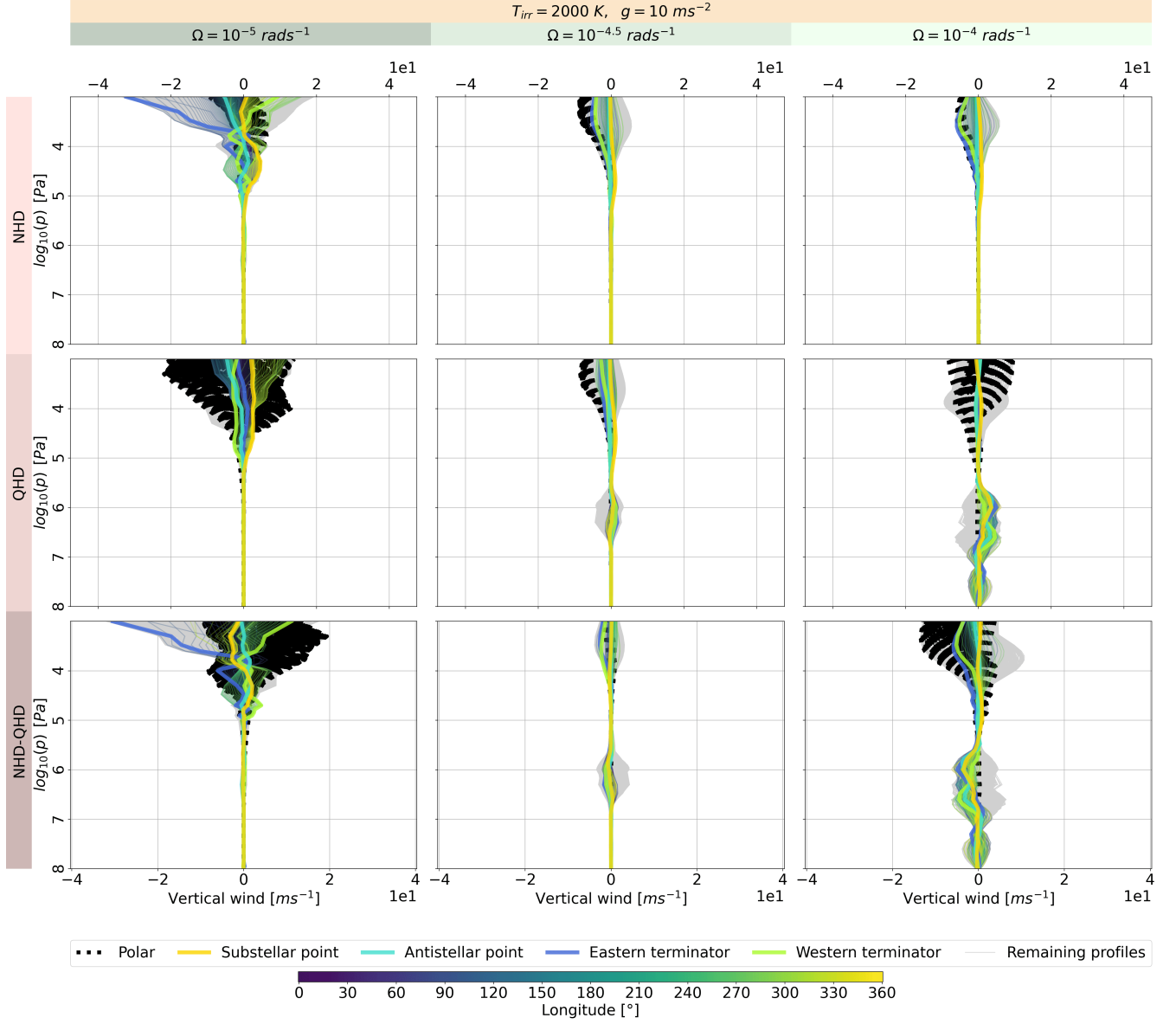


**Figure 12.** Vertical wind speed at each grid point for the NHD and QHD equation sets with  $g = 10 \text{ ms}^{-2}$ ,  $T_{irr} = 2'000 \text{ K}$  and with altering  $\Omega$ . The coloured lines indicate momenta profiles along the equator and its coordinates by the colourbar. The dotted black thin line shows momenta profiles at the latitudes  $87^\circ\text{N}$  and  $87^\circ\text{S}$ . The bold coloured lines represent momenta profiles at the western, eastern terminators, sub- and antistellar point. The grey lines represents all the other momenta profiles.

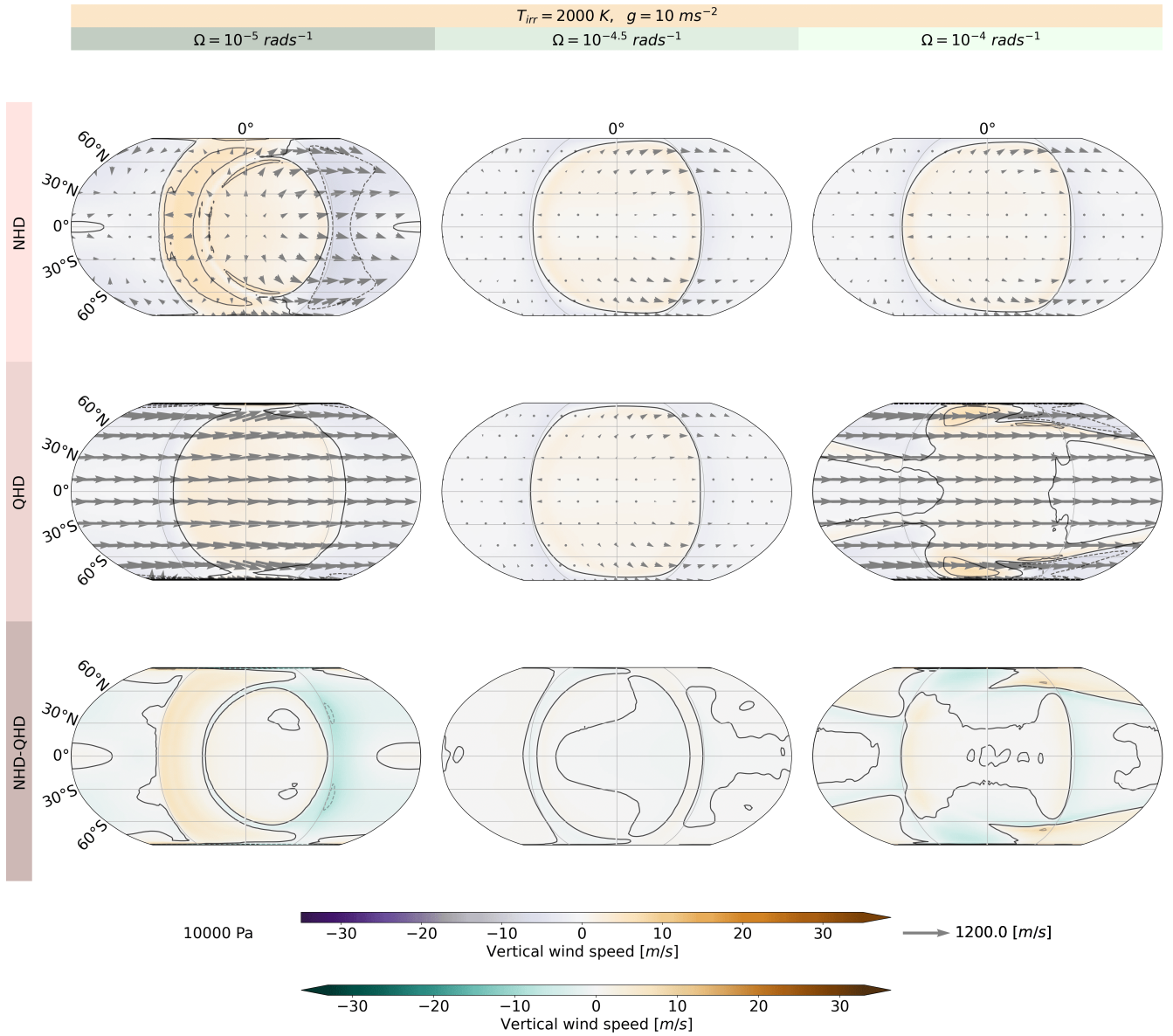


**Figure 13.** Vertical wind speed at 10'000 Pa for the NHD and QHD equation sets with  $g = 10 \text{ ms}^{-2}$ ,  $T_{irr} = 2'000 \text{ K}$  and with altering  $\Omega$ . The arrows indicate the horizontal wind speed



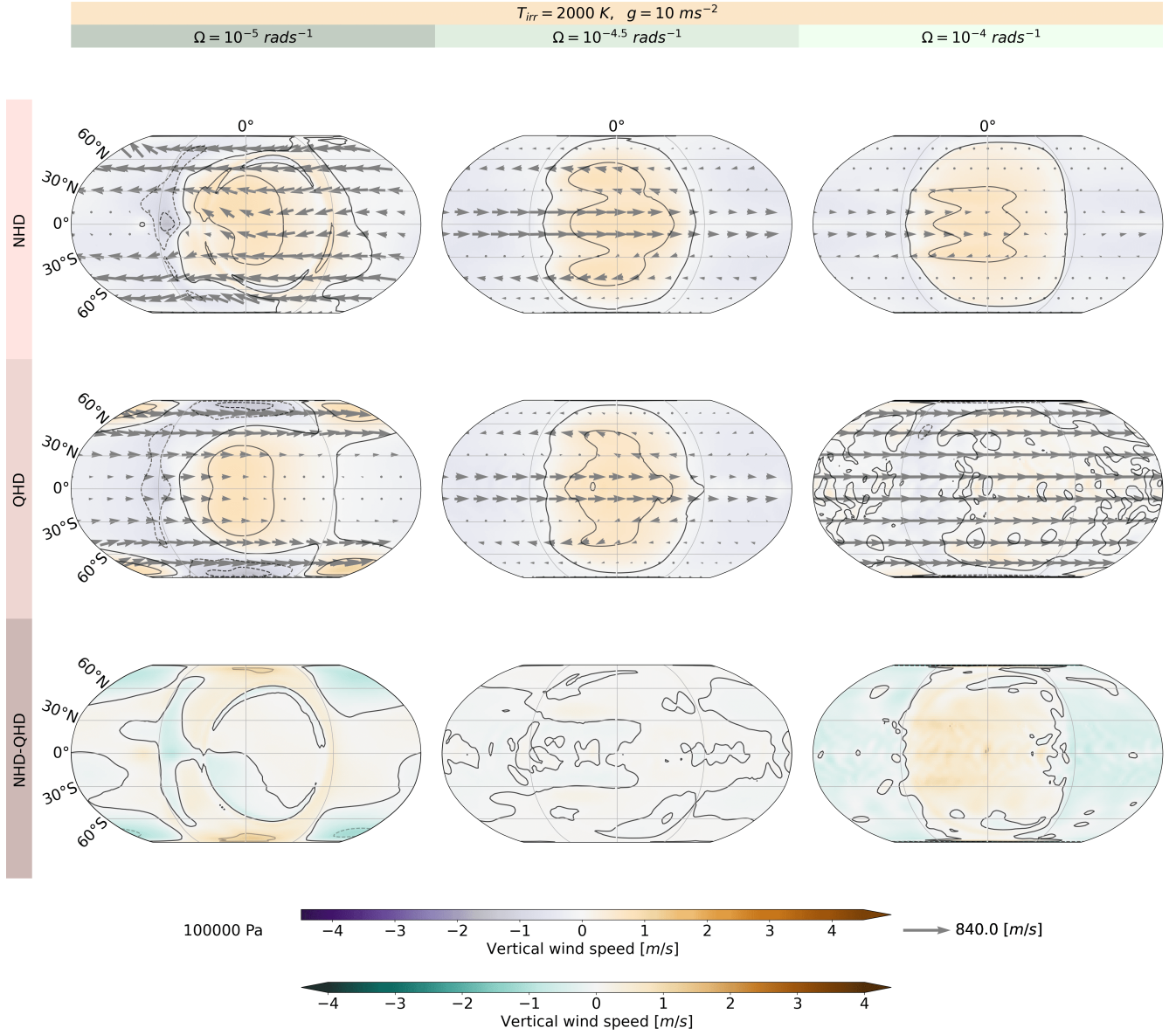


**Figure 14.** Vertical wind speed at 100'000 Pa for the NHD and QHD equation sets with  $g = 10 \text{ ms}^{-2}$ ,  $T_{irr} = 2'000 \text{ K}$  and with altering  $\Omega$ . The arrows indicate the horizontal wind speed

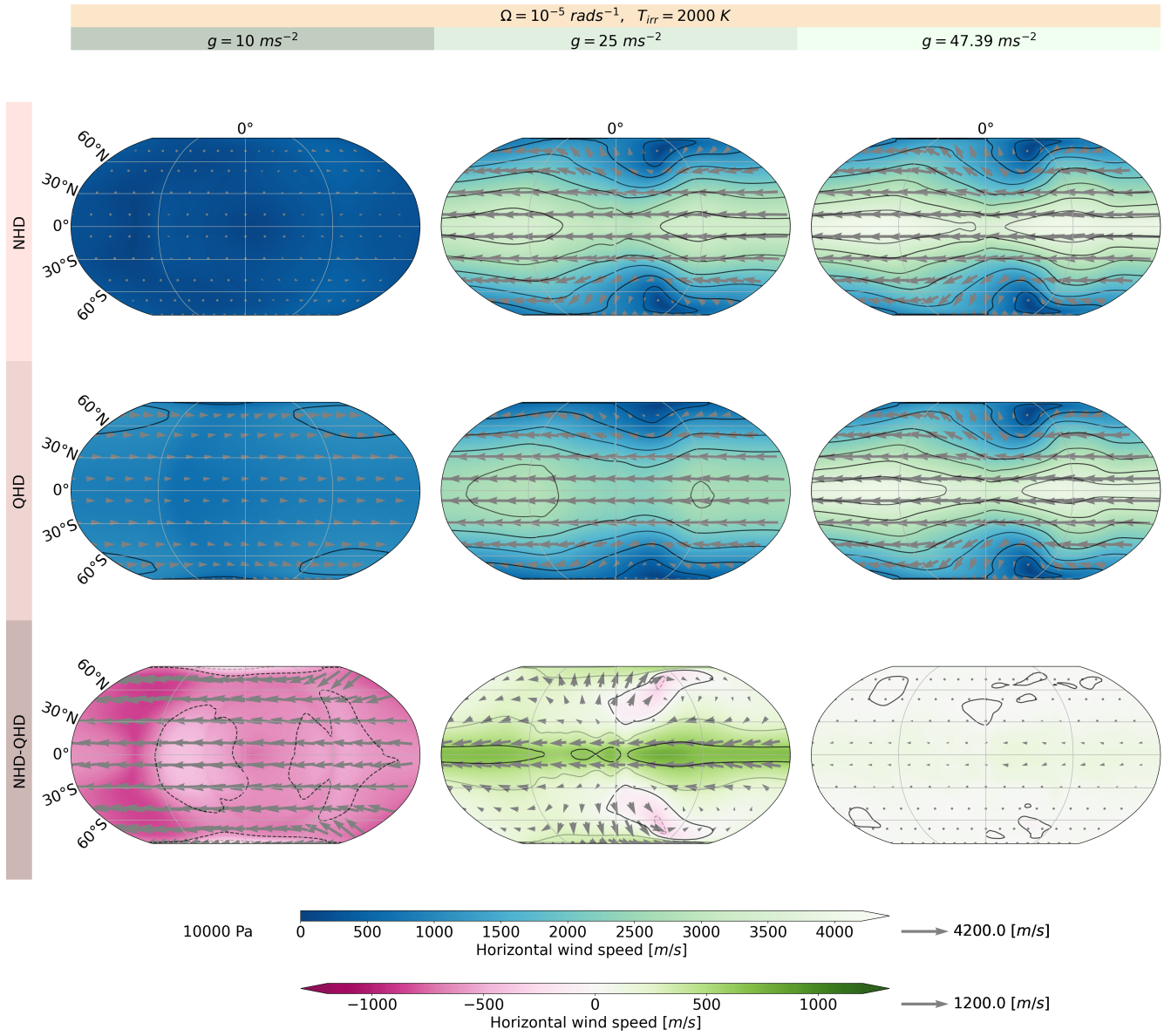


**Figure 15.** Horizontal wind speed at 10'000 Pa for the NHD and QHD equation sets with  $\Omega = 1 \cdot 10^{-5} \text{ rad/s}$ ,  $T_{irr} = 2'000 \text{ K}$  and with altering  $g$ .



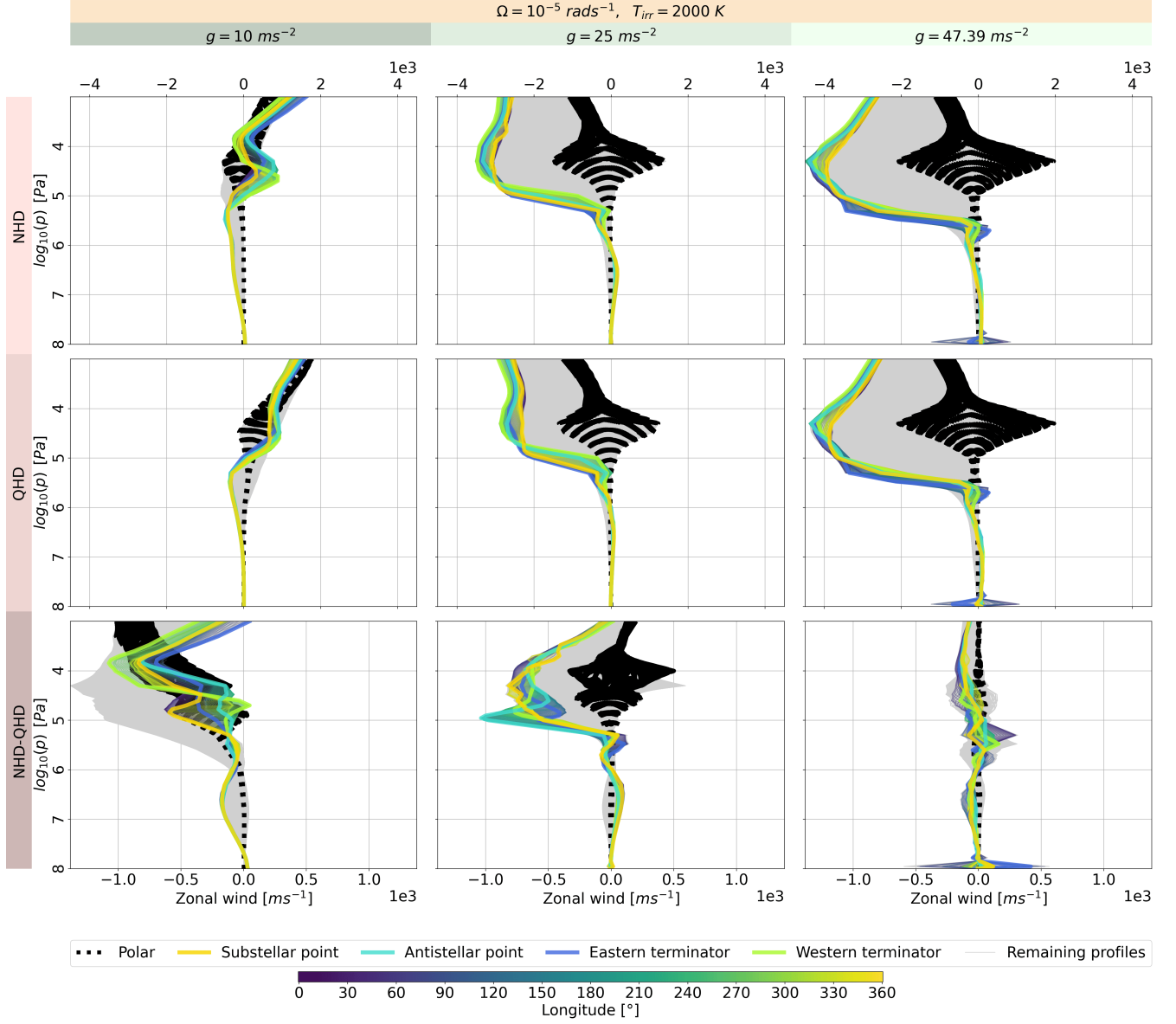


**Figure 16.** Zonal wind speed at each grid point for the NHD and QHD equation sets with  $\Omega = 1 \cdot 10^{-5} \text{ rad/s}$ ,  $T_{\text{irr}} = 2'000 \text{ K}$  and with altering  $g$ . The coloured lines indicate momenta profiles along the equator and its coordinates by the colourbar. The dotted black thin line shows momenta profiles at the latitudes  $87^\circ\text{N}$  and  $87^\circ\text{S}$ . The bold coloured lines represent momenta profiles at the western, eastern terminators, sub- and antistellar point. The grey lines represents all the other momenta profiles.

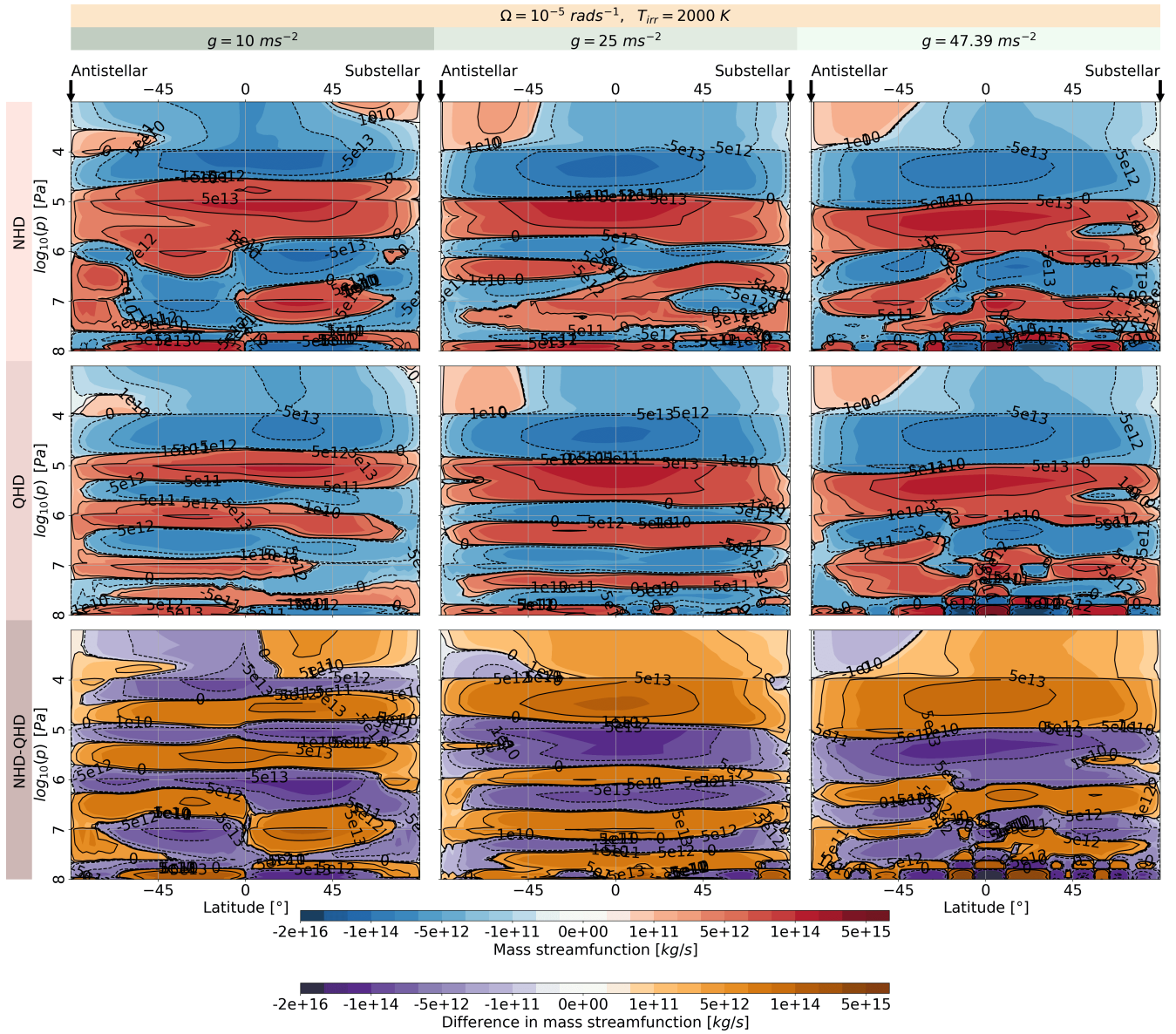


**Figure 17.** Overturning circulation depicted by the streamfunction  $\Psi'$  in tidally locked coordinates for the NHD and QHD equation sets with  $\Omega = 1 \cdot 10^{-5} \text{ rad/s}$ ,  $T_{\text{irr}} = 2'000 \text{ K}$  and with altering  $g$ .

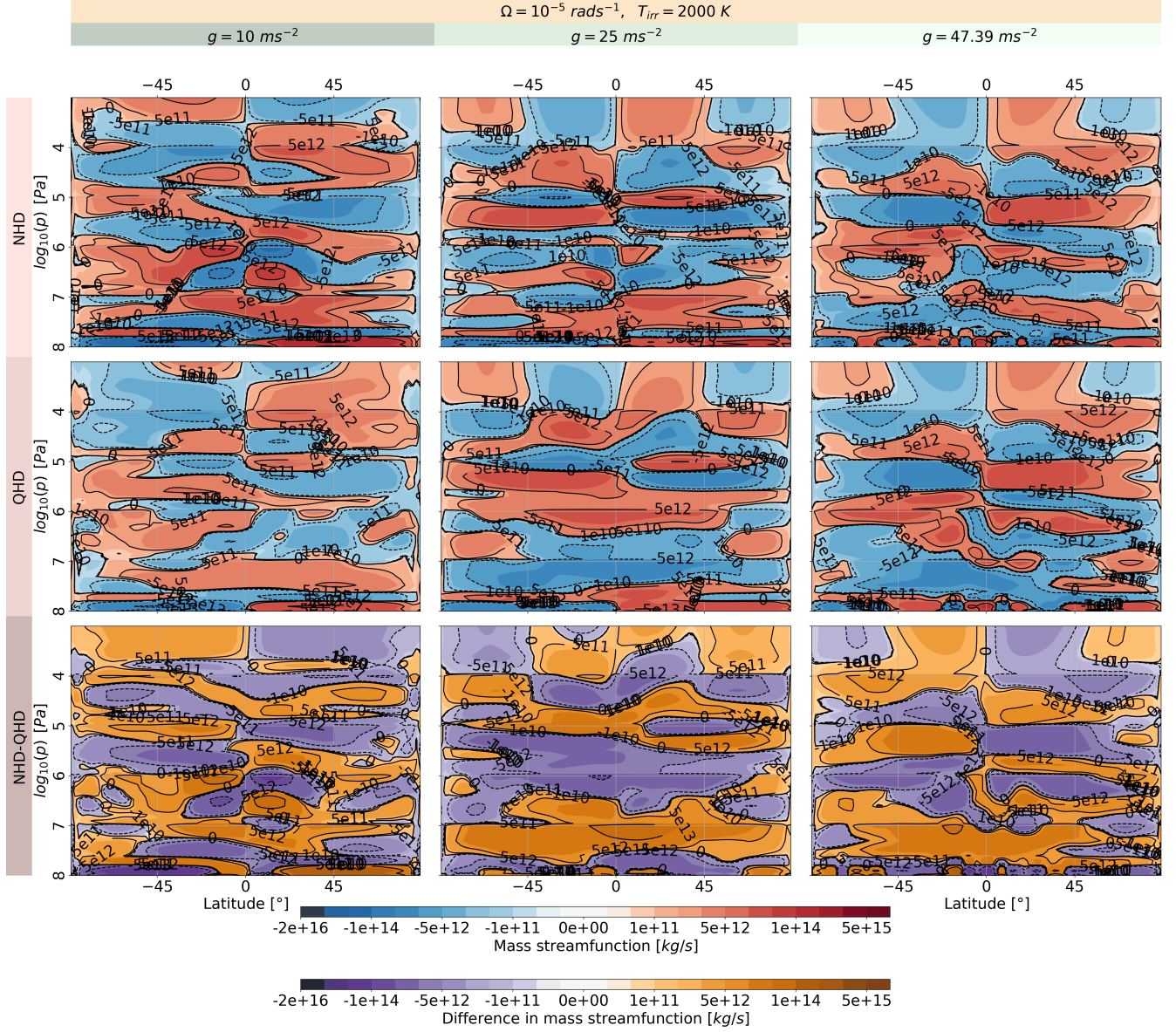


**Figure 18.** Overturning circulation depicted by the streamfunction  $\Psi$  for the NHD and QHD equation sets with  $\Omega = 1 \cdot 10^{-5} \text{ rad/s}$ ,  $T_{\text{irr}} = 2'000 \text{ K}$  and with altering  $g$ .

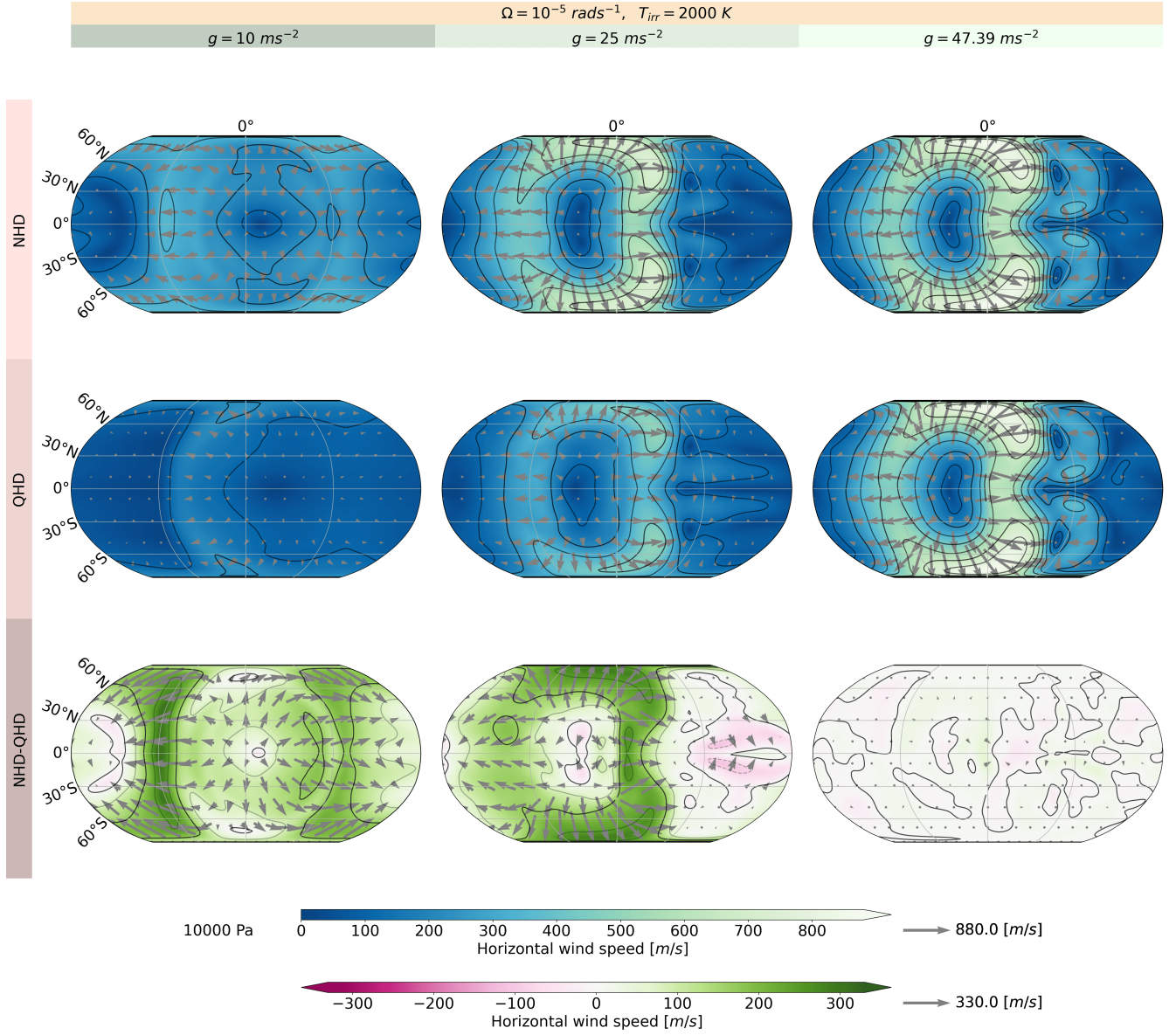


**Figure 19.** Divergent component of the Helmholtz decomposition at  $10'000 \text{ Pa}$  for the NHD and QHD equation sets with  $\Omega = 1 \cdot 10^{-5} \text{ rad/s}$ ,  $T_{irr} = 2'000 \text{ K}$  and with altering  $g$ .



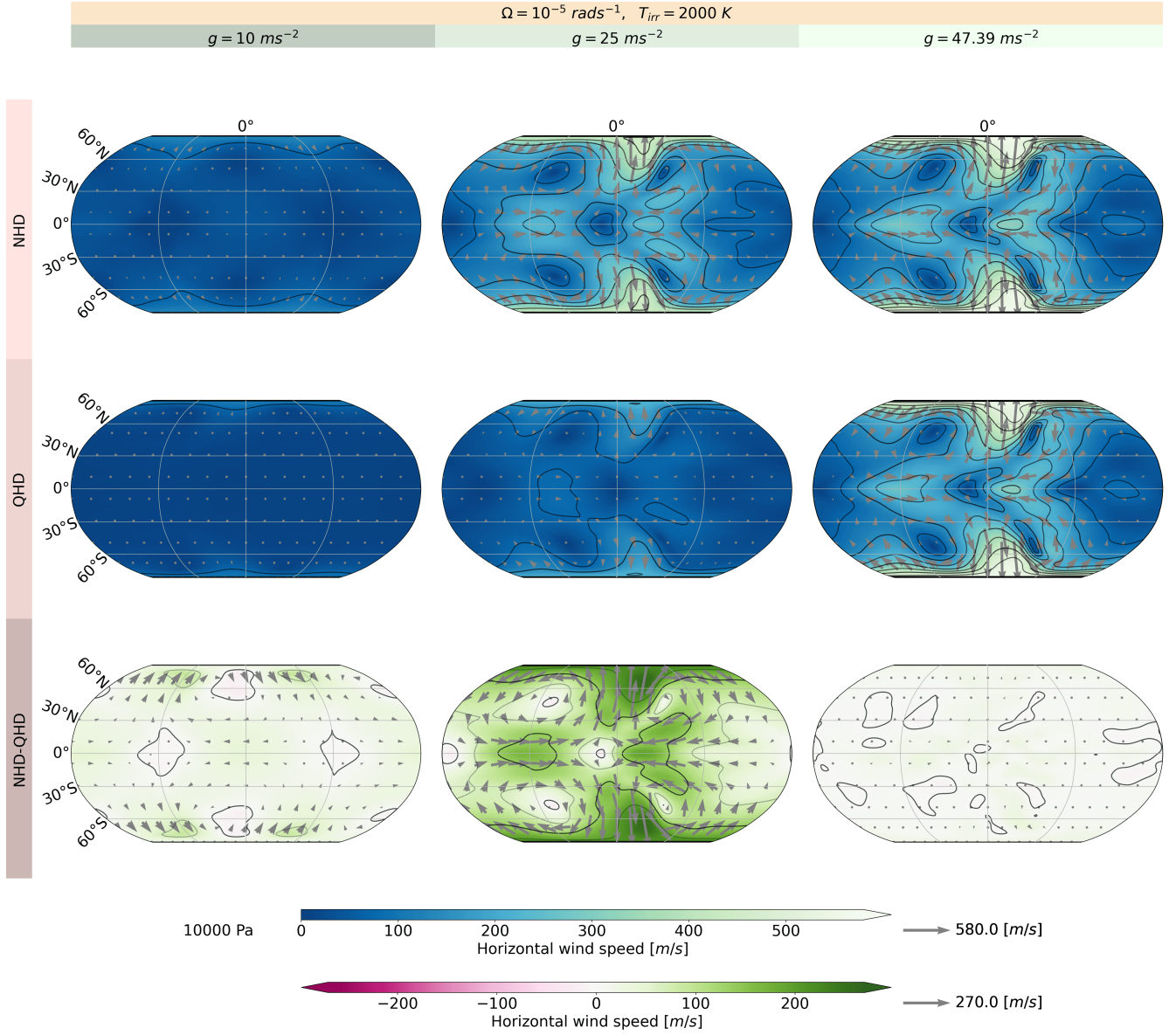


**Figure 20.** Rotational eddy component of the Helmholtz decomposition at 10'000 Pa for the NHD and QHD equation sets with  $\Omega = 1 \cdot 10^{-5} \text{ rad/s}$ ,  $T_{irr} = 2'000 \text{ K}$  and with altering  $g$ .

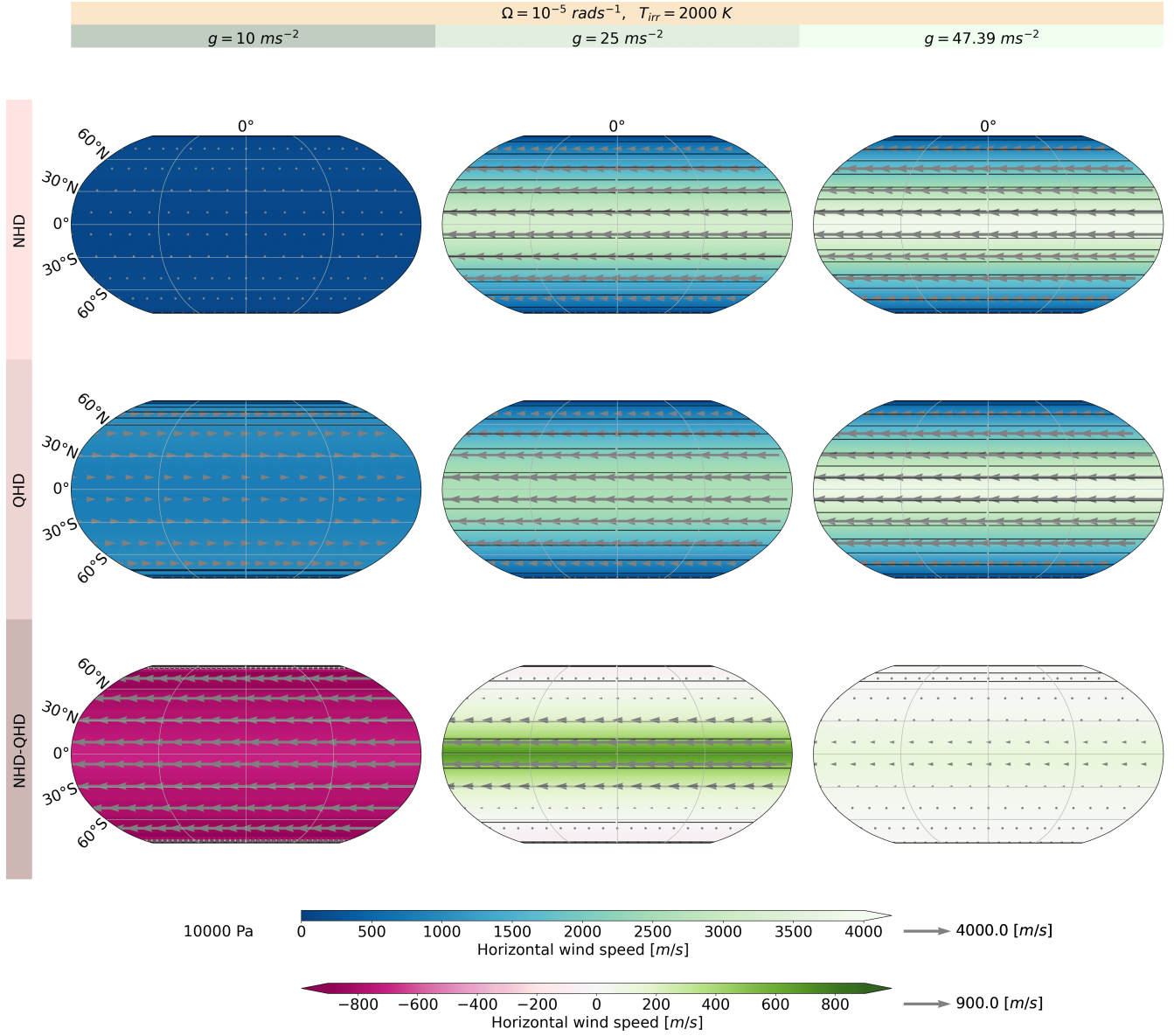


**Figure 21.** Rotational jet component of the Helmholtz decomposition at  $10'000 \text{ Pa}$  for the NHD and QHD equation sets with  $\Omega = 1 \cdot 10^{-5} \text{ rad/s}$ ,  $T_{\text{irr}} = 2'000 \text{ K}$  and with altering  $g$ .

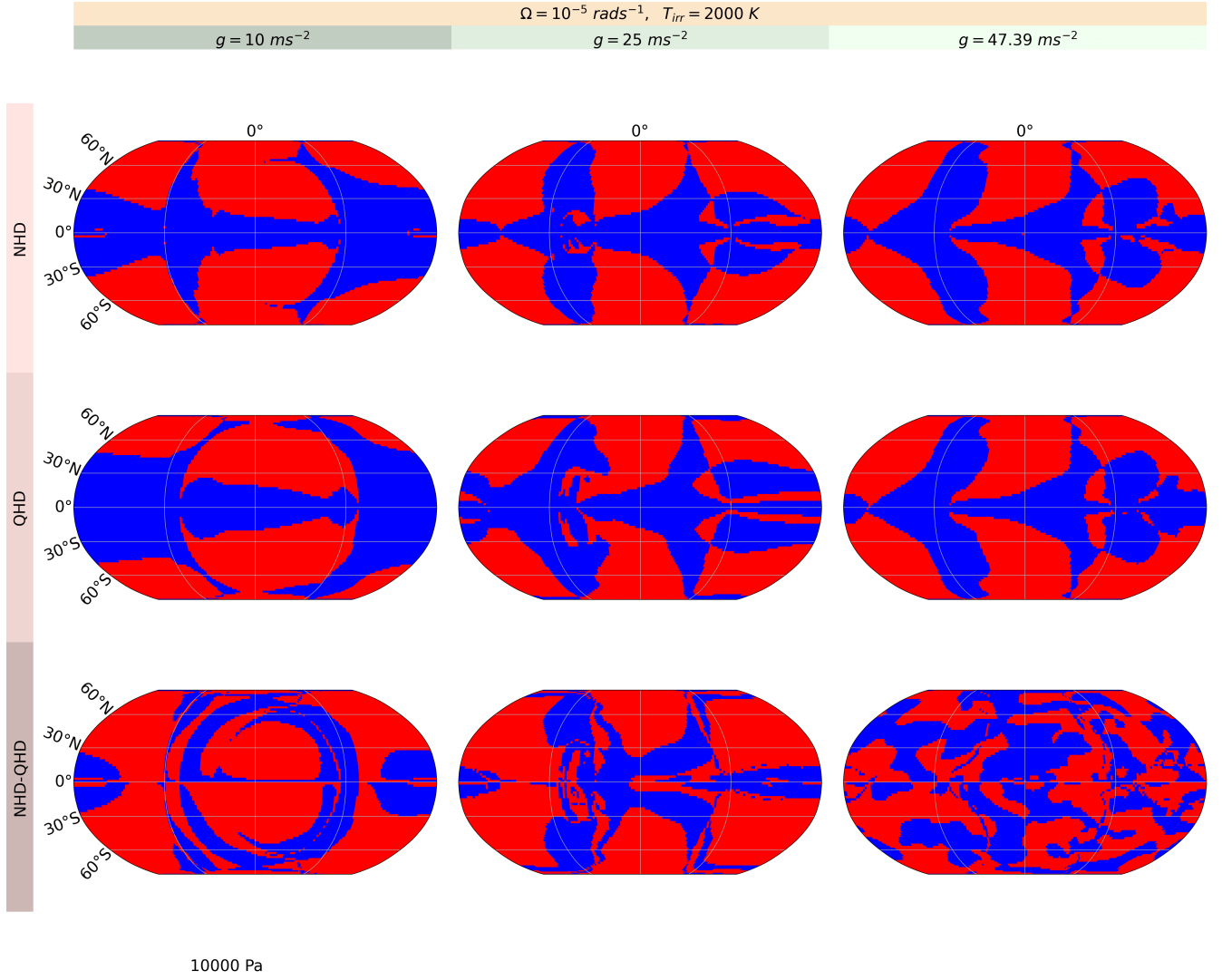


**Figure 22.** Sign of  $\frac{v \tan(\Phi)}{10w} - 1$  for the NHD and QHD equation sets with  $\Omega = 1 \cdot 10^{-5} \text{ rad/s}$ ,  $T_{irr} = 2'000 \text{ K}$  and with altering  $g$ . Dark blue and bright blue regions show negative and positive values



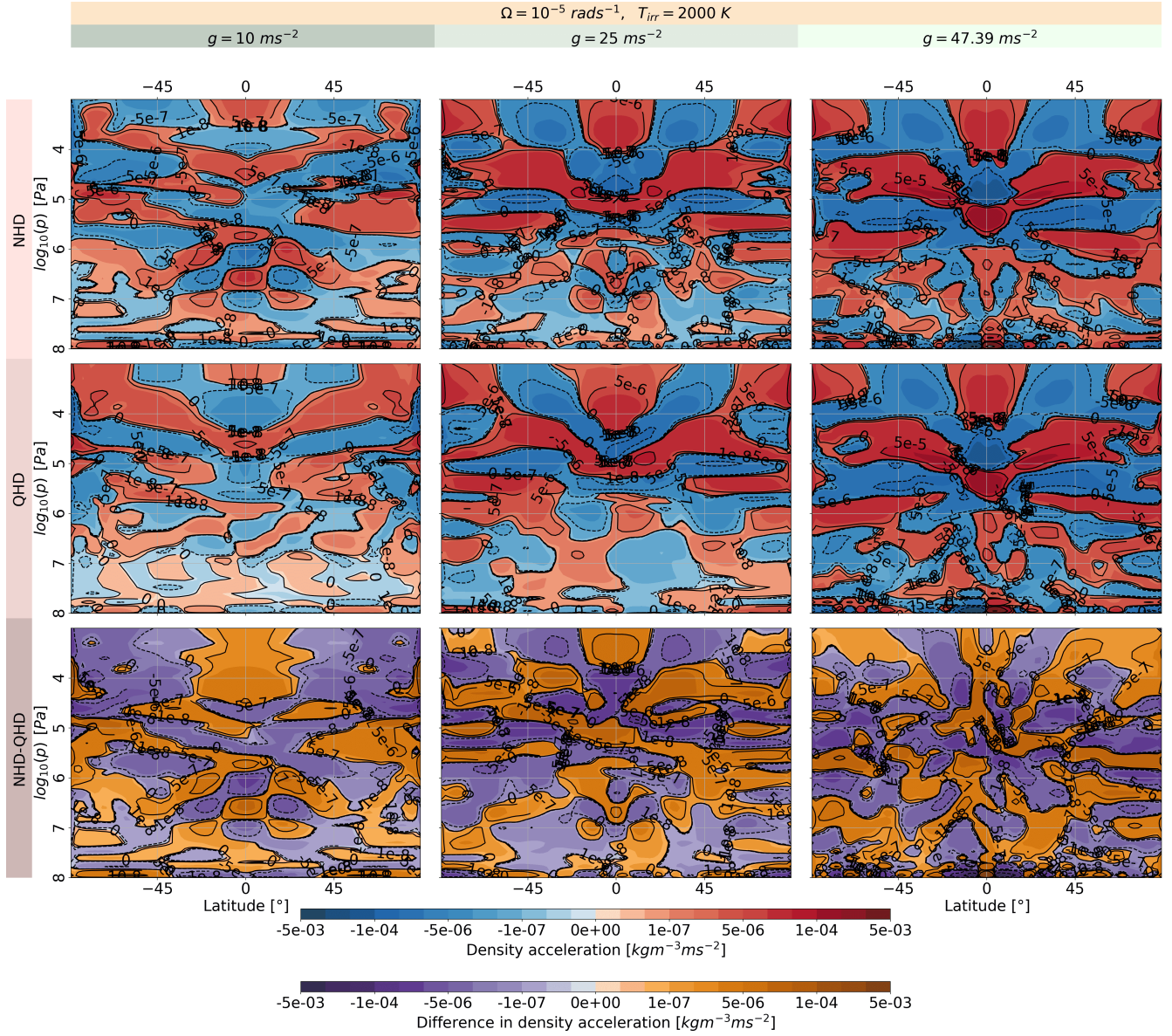


**Figure 23.** Horizontal acceleration for the NHD and QHD equation sets with  $\Omega = 1 \cdot 10^{-5} \text{ rad/s}$ ,  $T_{\text{irr}} = 2'000 \text{ K}$  and with altering  $g$ .

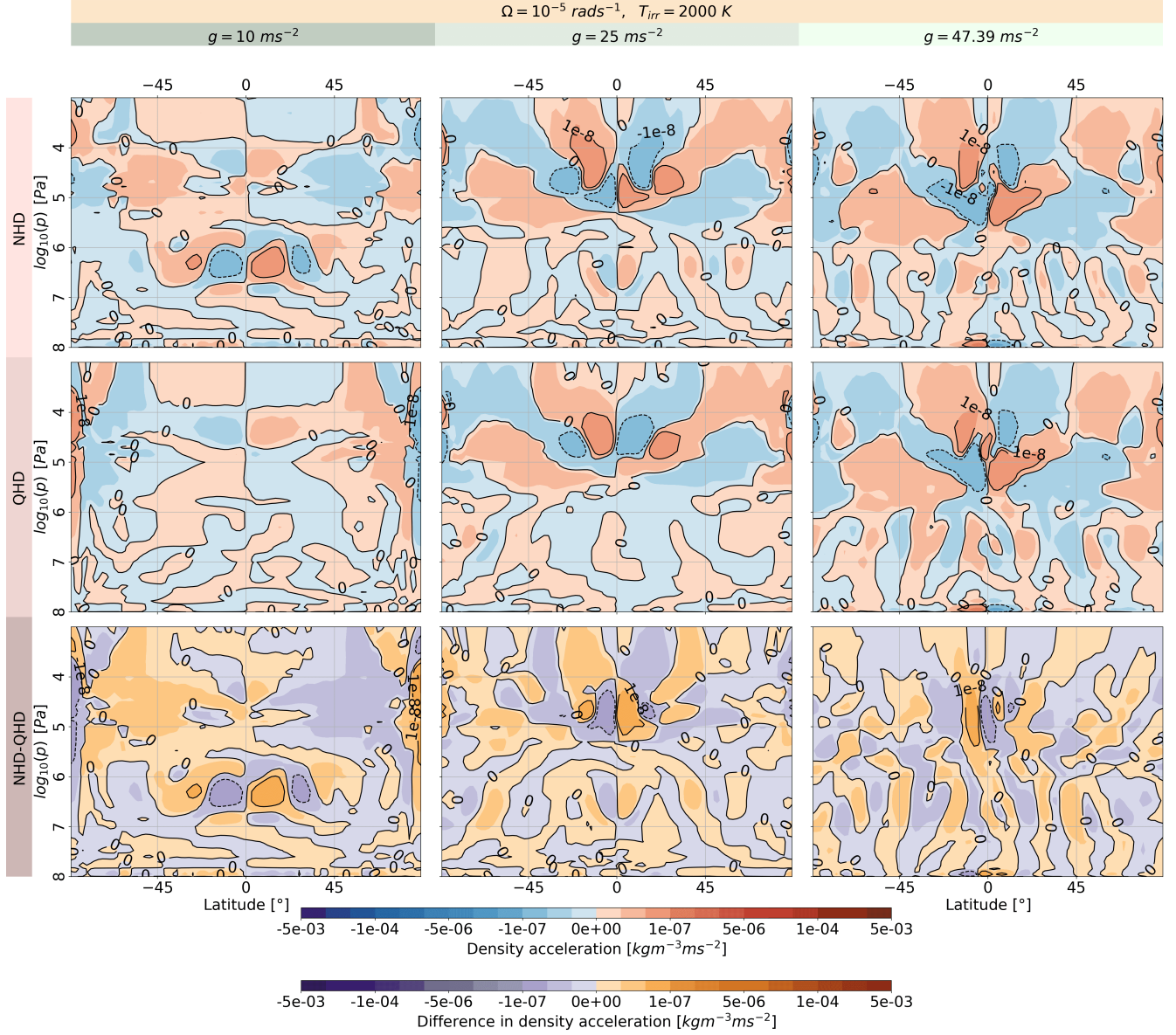


**Figure 24.** Vertical acceleration for the NHD and QHD equation sets with  $\Omega = 1 \cdot 10^{-5} \text{ rad/s}$ ,  $T_{\text{irr}} = 2'000 \text{ K}$  and with altering  $g$ .

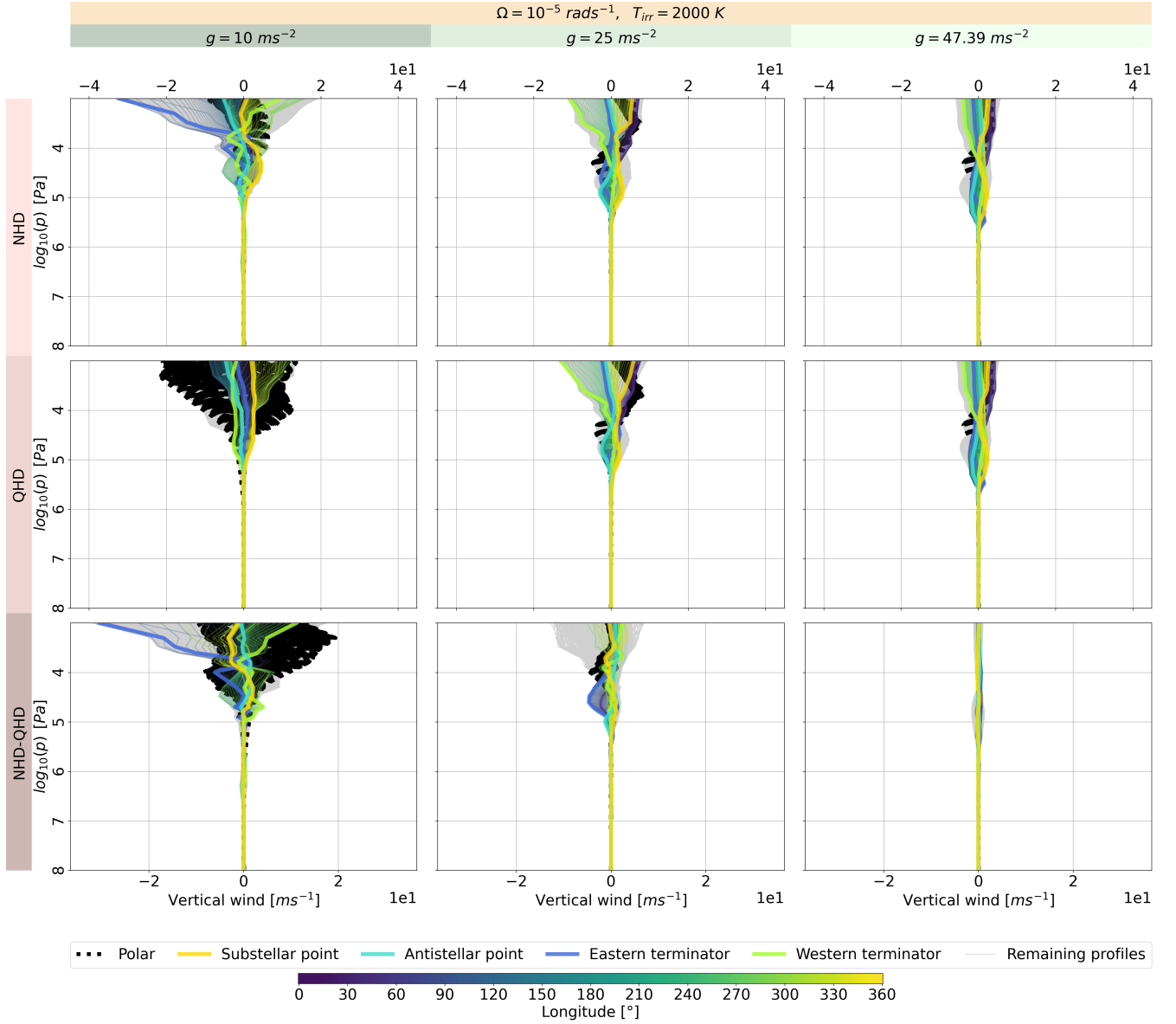


**Figure 25.** Vertical wind speed at each grid point for the NHD and QHD equation sets with  $\Omega = 1 \cdot 10^{-5} \text{ rad/s}$ ,  $T_{\text{irr}} = 2'000 \text{ K}$  and with altering  $g$ . The coloured lines indicate momenta profiles along the equator and its coordinates by the colourbar. The dotted black thin line shows momenta profiles at the latitudes  $87^{\circ}\text{N}$  and  $87^{\circ}\text{S}$ . The bold coloured lines represent momenta profiles at the western, eastern terminators, sub- and antistellar point. The grey lines represents all the other momenta profiles.

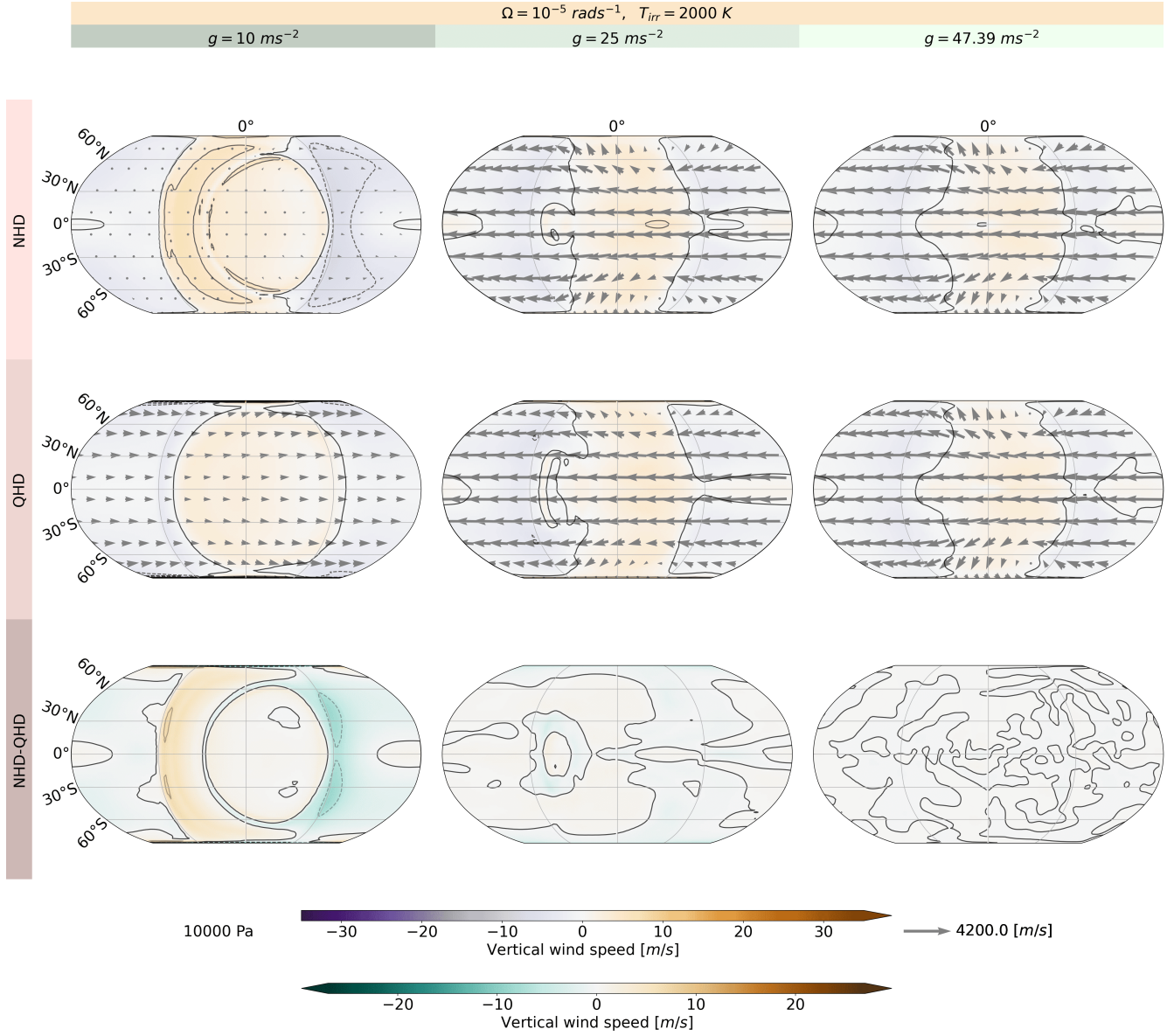


**Figure 26.** Vertical wind speed at 10'000 Pa for the NHD and QHD equation sets with  $\Omega = 1 \cdot 10^{-5} \text{ rad/s}$ ,  $T_{irr} = 2'000 \text{ K}$  and with altering  $g$ . The arrows indicate the horizontal wind speed



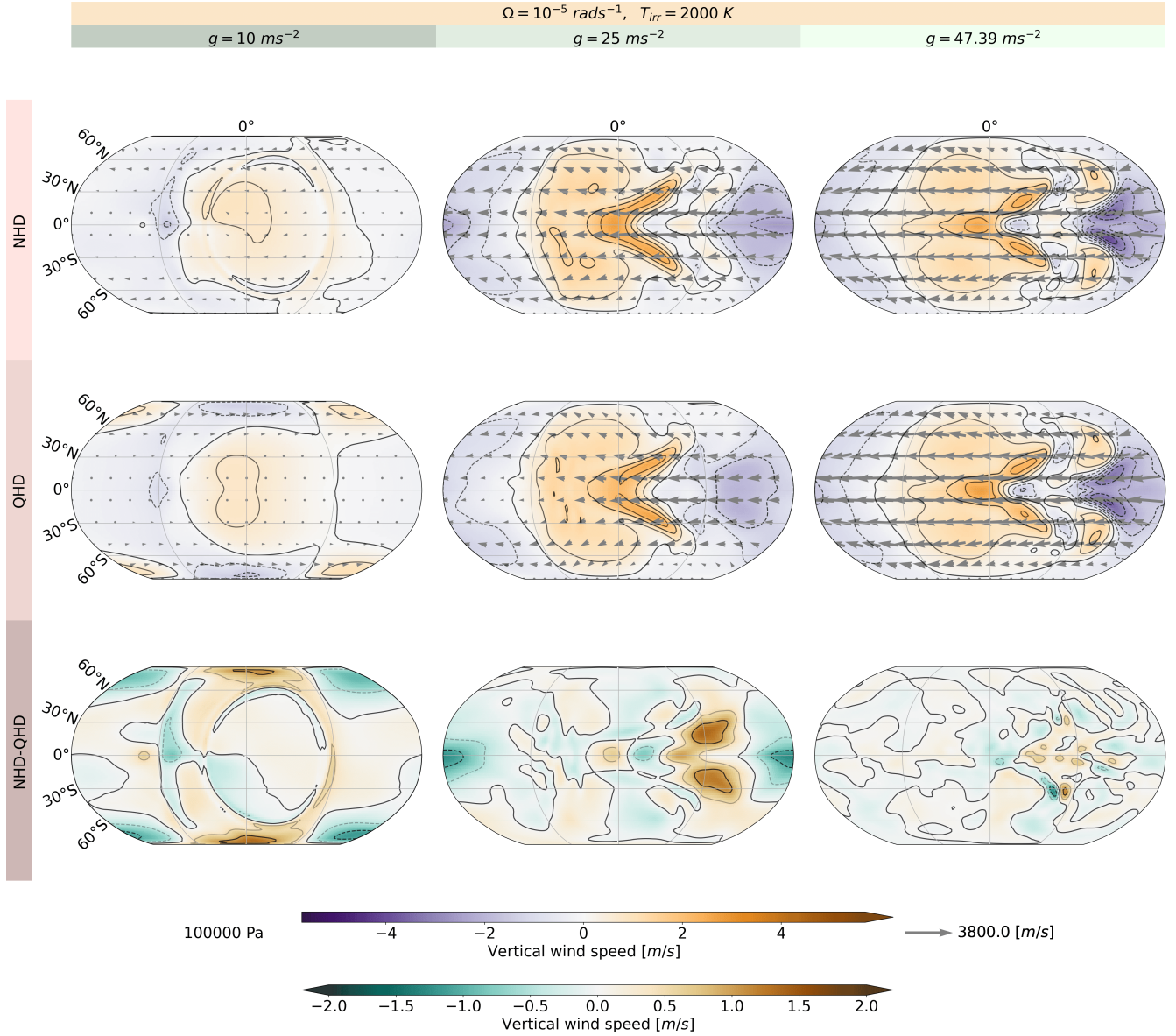


**Figure 27.** Vertical wind speed at 100'000 Pa for the NHD and QHD equation sets with  $\Omega = 1 \cdot 10^{-5} \text{ rad/s}$ ,  $T_{\text{irr}} = 2'000 \text{ K}$  and with altering  $g$ . The arrows indicate the horizontal wind speed

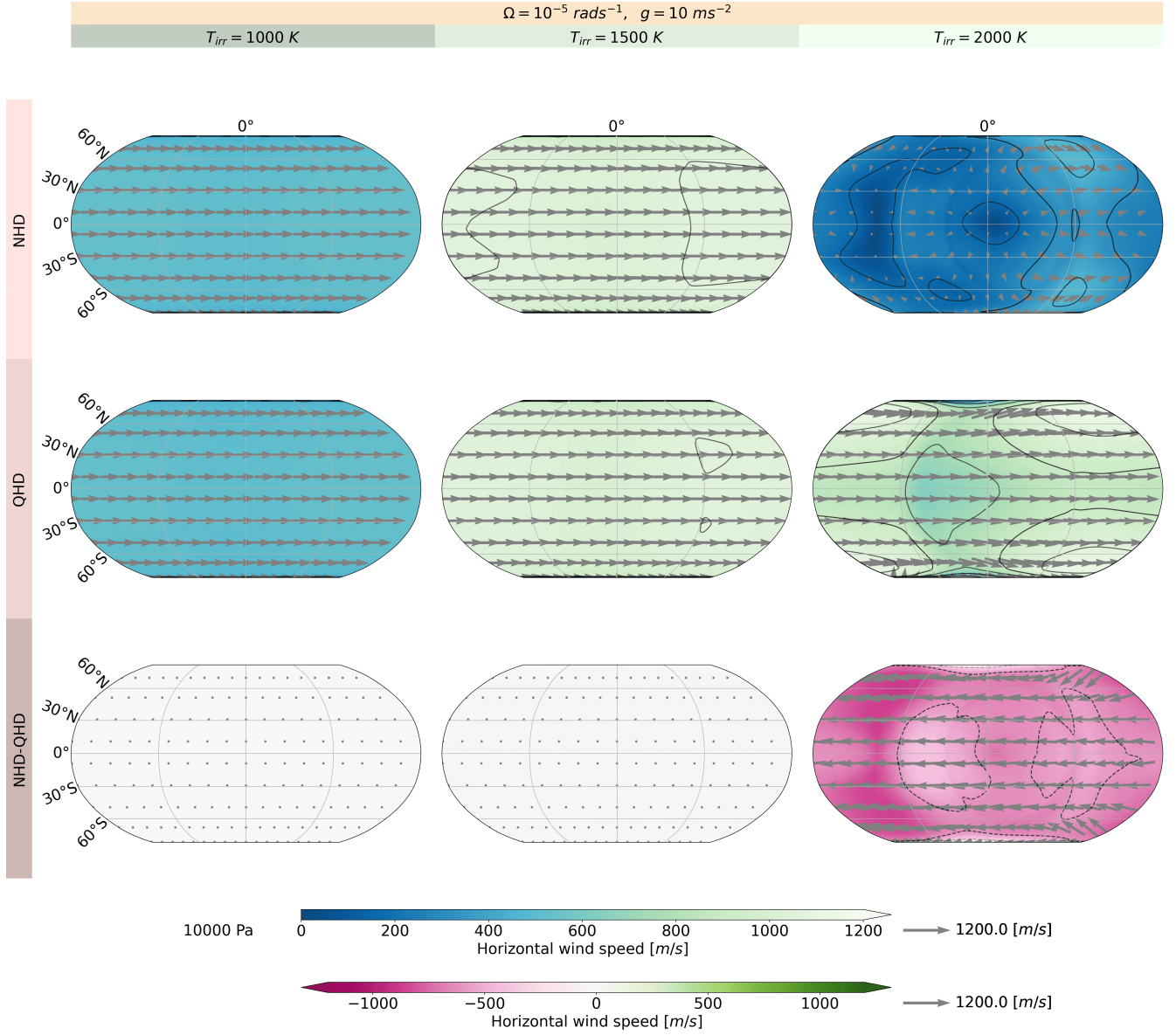


**Figure 28.** Horizontal wind speed at 10'000 Pa for the NHD and QHD equation sets with  $g = 10\text{ ms}^{-2}$ ,  $\Omega = 1 \cdot 10^{-5}\text{ rad/s}$  and with altering  $T_{irr}$ .

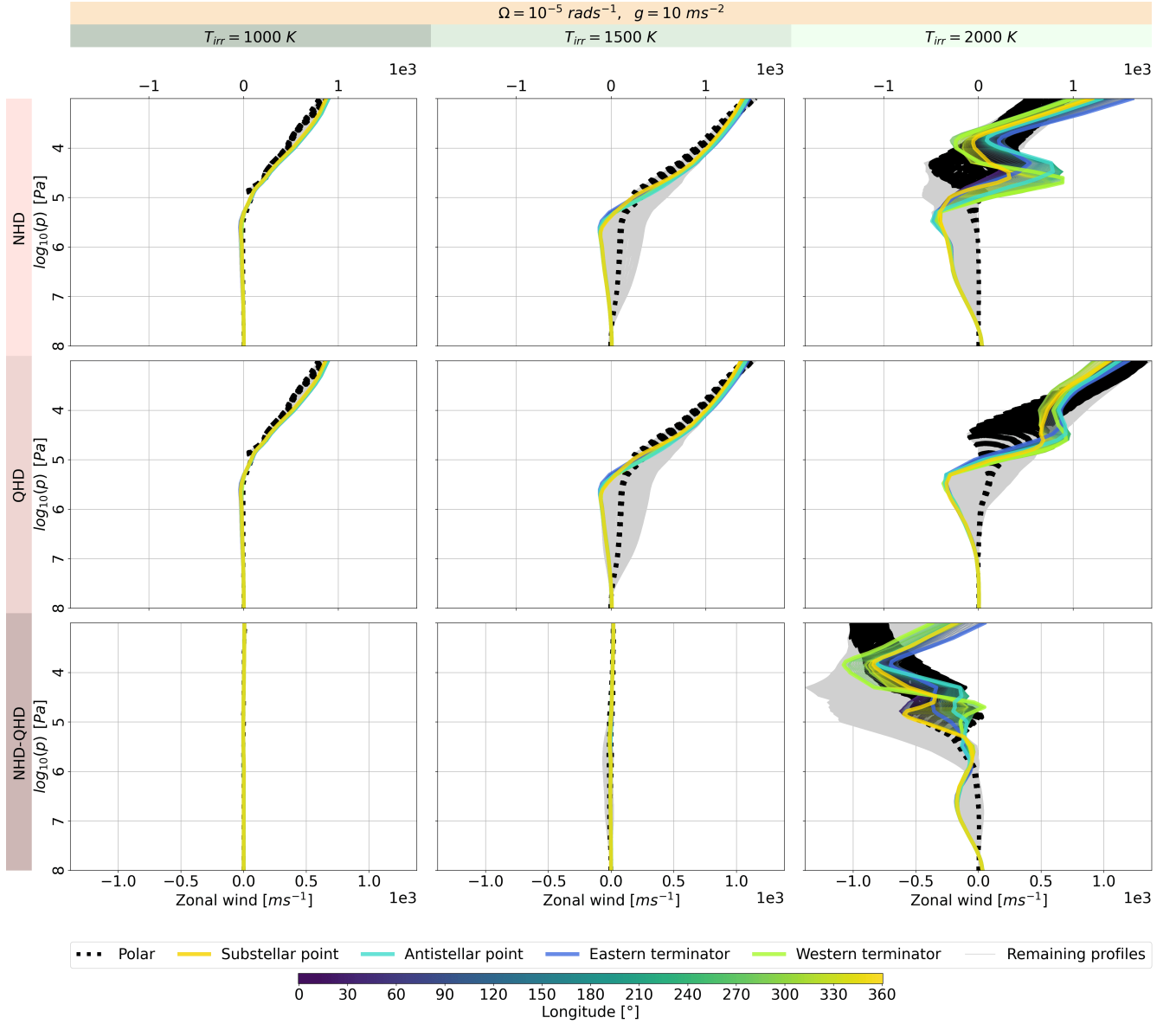


**Figure 29.** Zonal wind speed at each grid point for the NHD and QHD equation sets with  $g = 10\text{ ms}^{-2}$ ,  $\Omega = 1 \cdot 10^{-5}\text{ rad/s}$  and with altering  $T_{irr}$ . The coloured lines indicate momenta profiles along the equator and its coordinates by the colourbar. The dotted black thin line shows momenta profiles at the latitudes  $87^\circ\text{N}$  and  $87^\circ\text{S}$ . The bold coloured lines represent momenta profiles at the western, eastern terminators, sub- and antistellar point. The grey lines represents all the other momenta profiles.



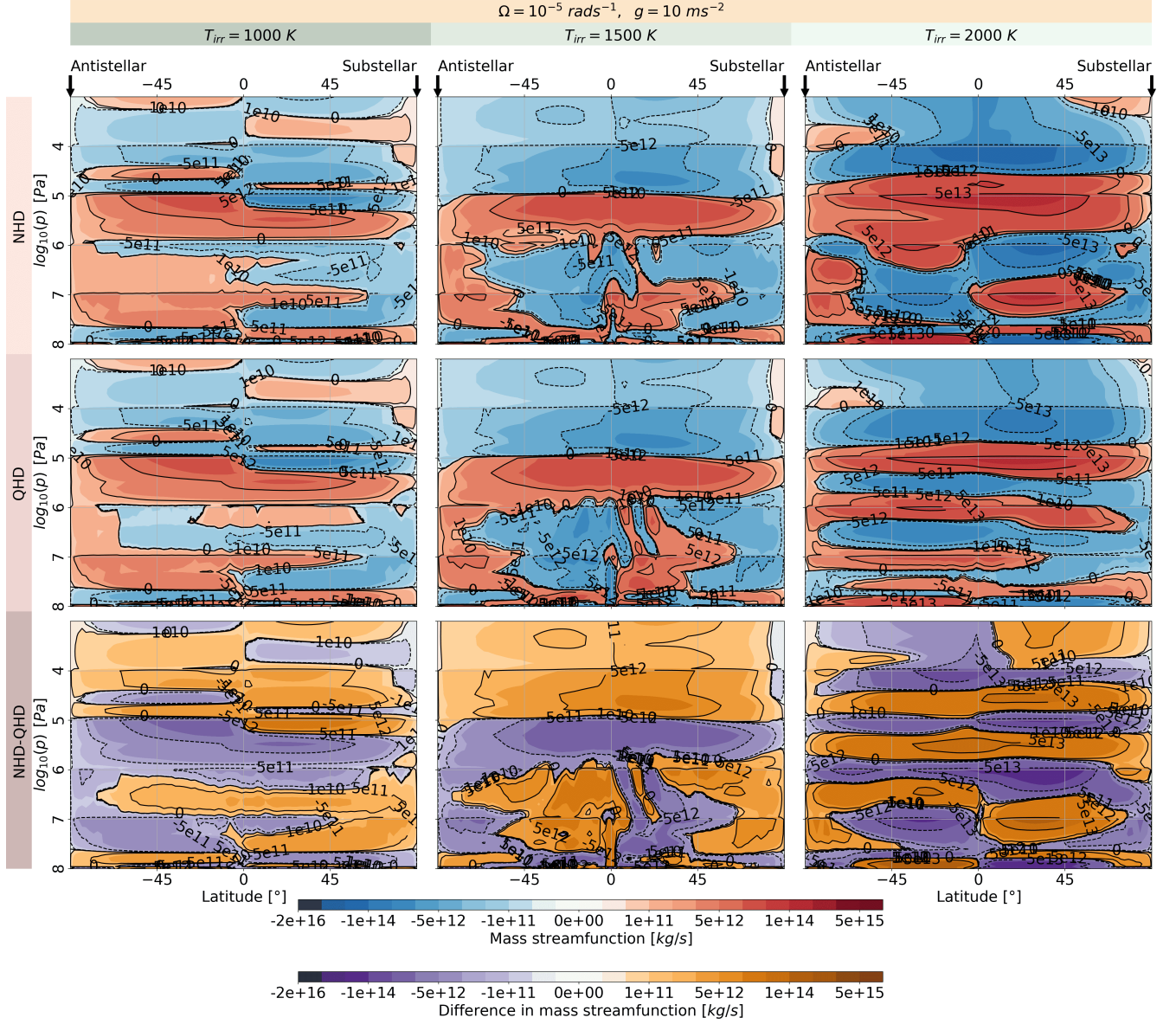


**Figure 30.** Overturning circulation depicted by the streamfunction  $\Psi'$  for the NHD and QHD equation sets with  $g = 10 \text{ ms}^{-2}$ ,  $\Omega = 1 \cdot 10^{-5} \text{ rad/s}$  and with altering  $T_{irr}$ .

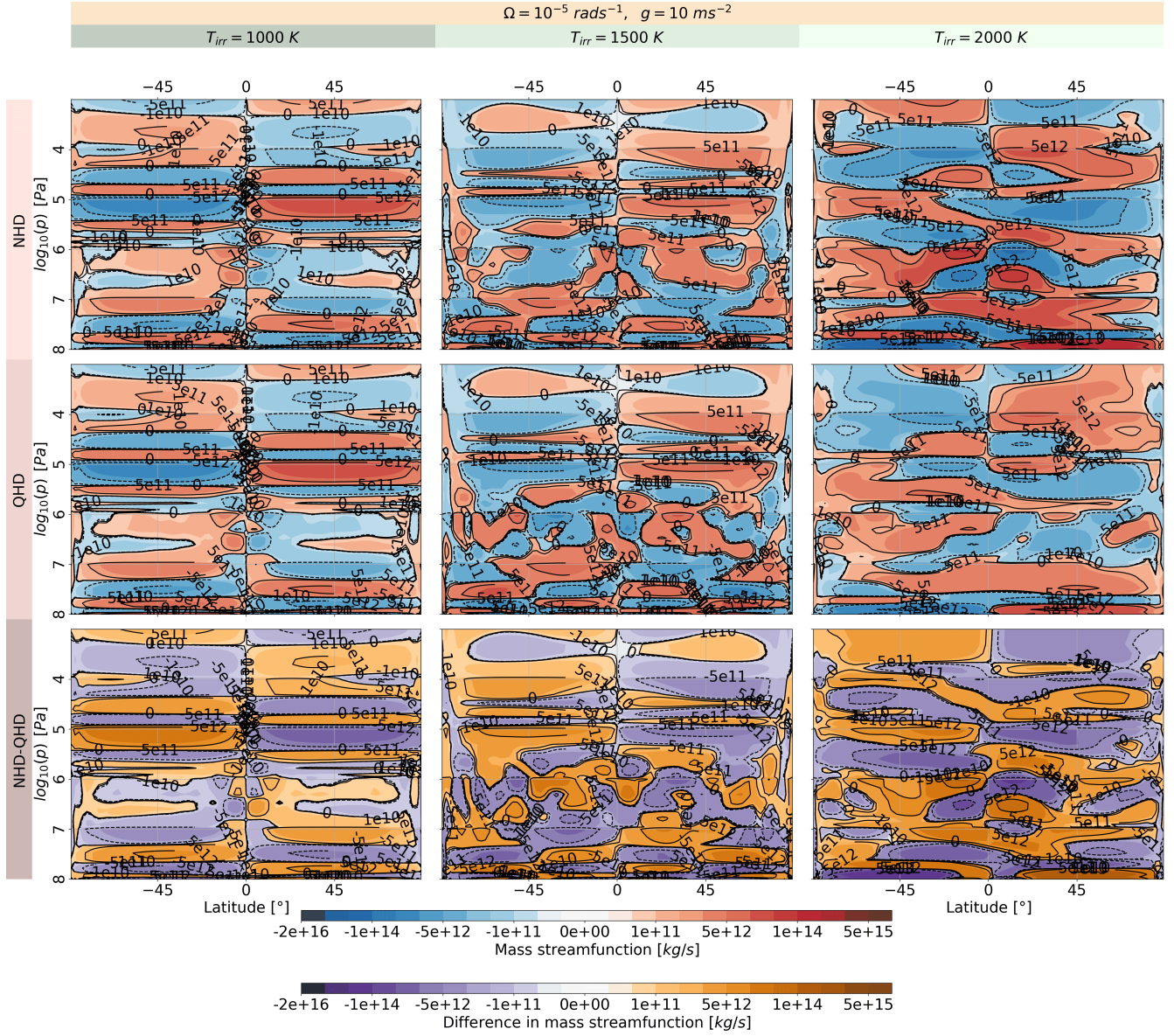


**Figure 31.** Overturning circulation depicted by the streamfunction  $\Psi$  for the NHD and QHD equation sets with  $g = 10 \text{ ms}^{-2}$ ,  $\Omega = 1 \cdot 10^{-5} \text{ rad/s}$  and with altering  $T_{\text{irr}}$ .

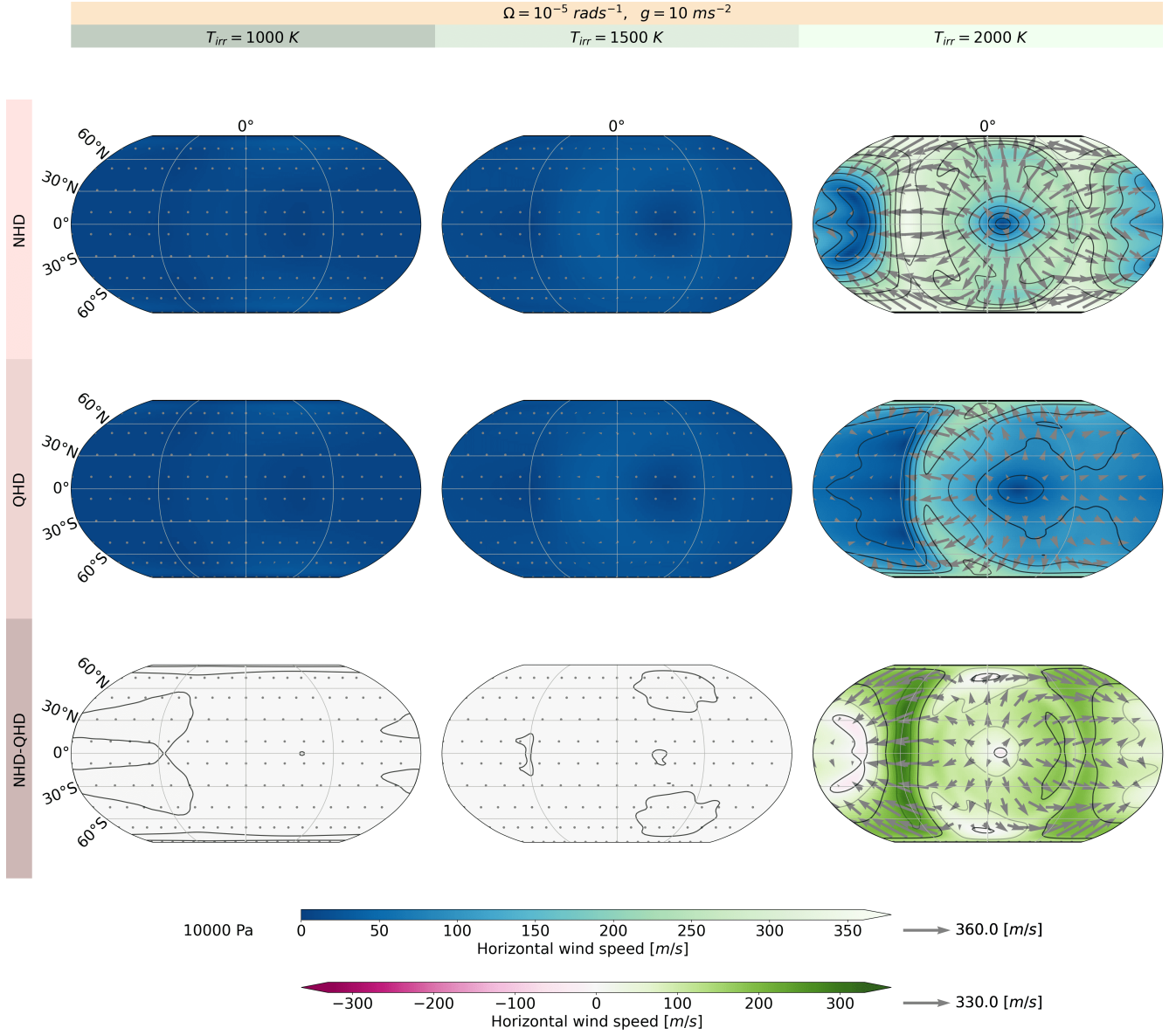


**Figure 32.** Divergent component of the Helmholtz decomposition for the NHD and QHD equation sets with  $g = 10 \text{ ms}^{-2}$ ,  $\Omega = 1 \cdot 10^{-5} \text{ rad/s}$  and with altering  $T_{irr}$ .



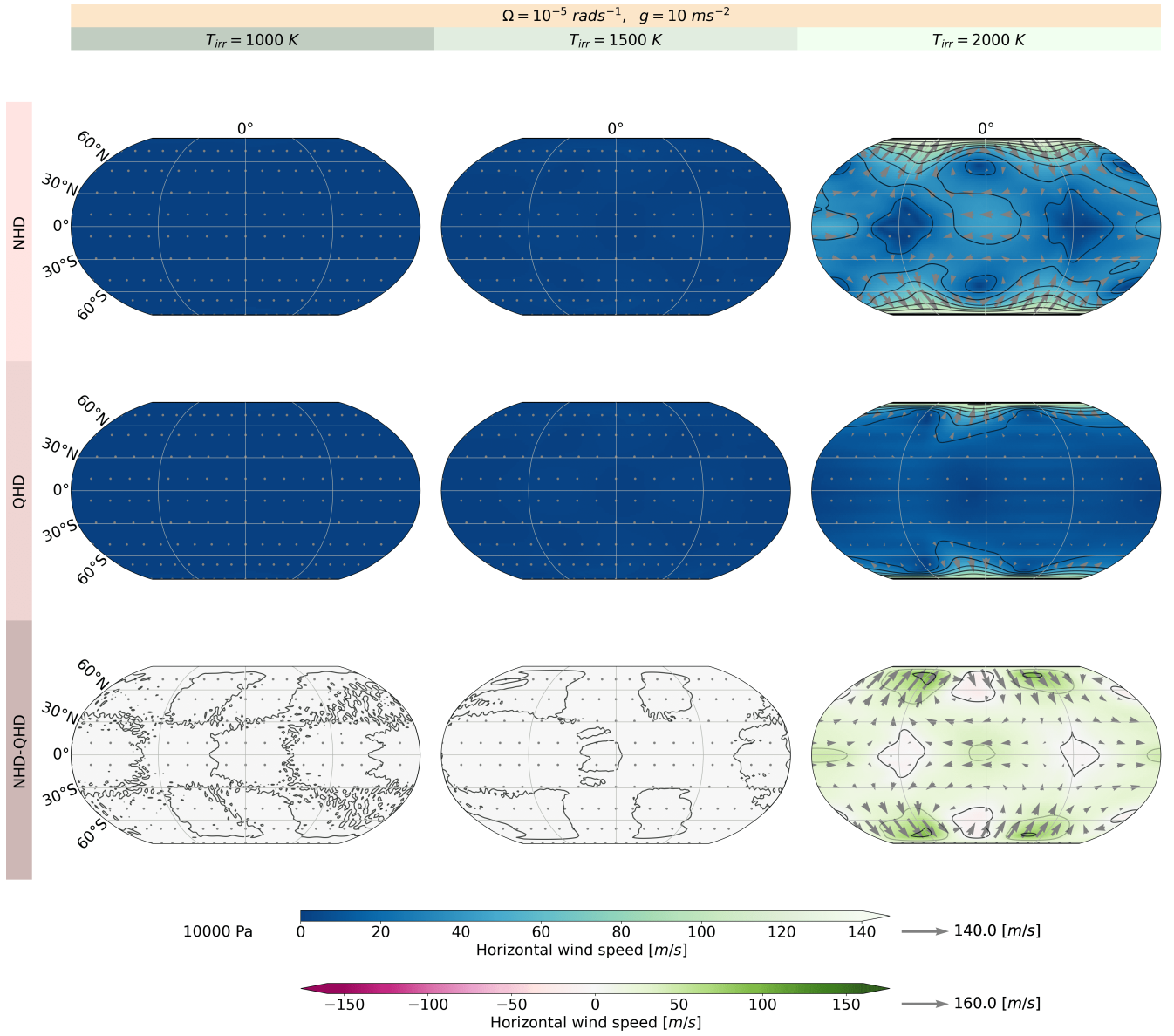


**Figure 33.** Rotational eddy component of the Helmholtz decomposition for the NHD and QHD equation sets with  $g = 10 \text{ ms}^{-2}$ ,  $\Omega = 1 \cdot 10^{-5} \text{ rad/s}$  and with altering  $T_{irr}$ .



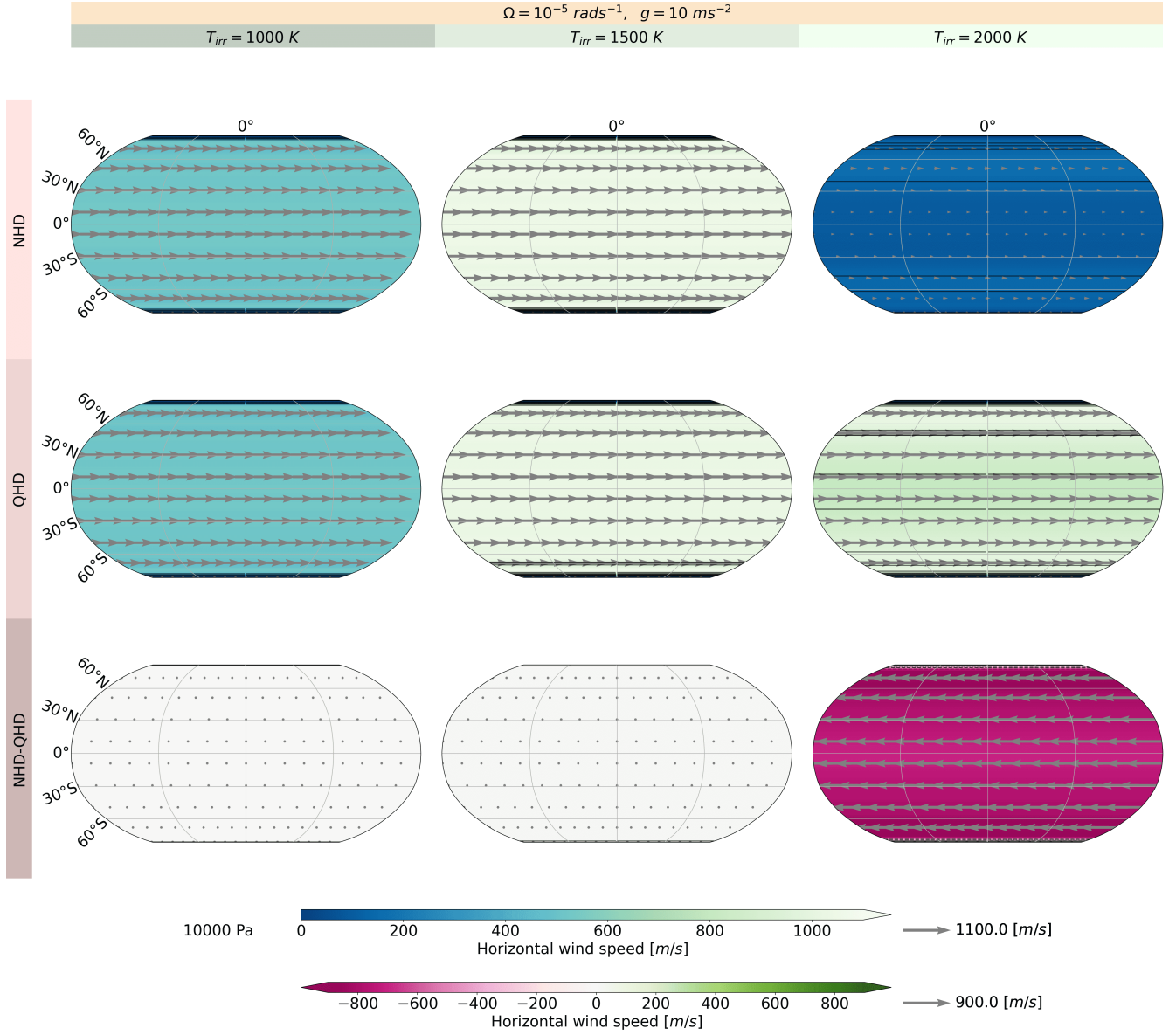


**Figure 34.** Rotational jet component of the Helmholtz decomposition for the NHD and QHD equation sets with  $g = 10 \text{ ms}^{-2}$ ,  $\Omega = 1 \cdot 10^{-5} \text{ rad/s}$  and with altering  $T_{irr}$ .

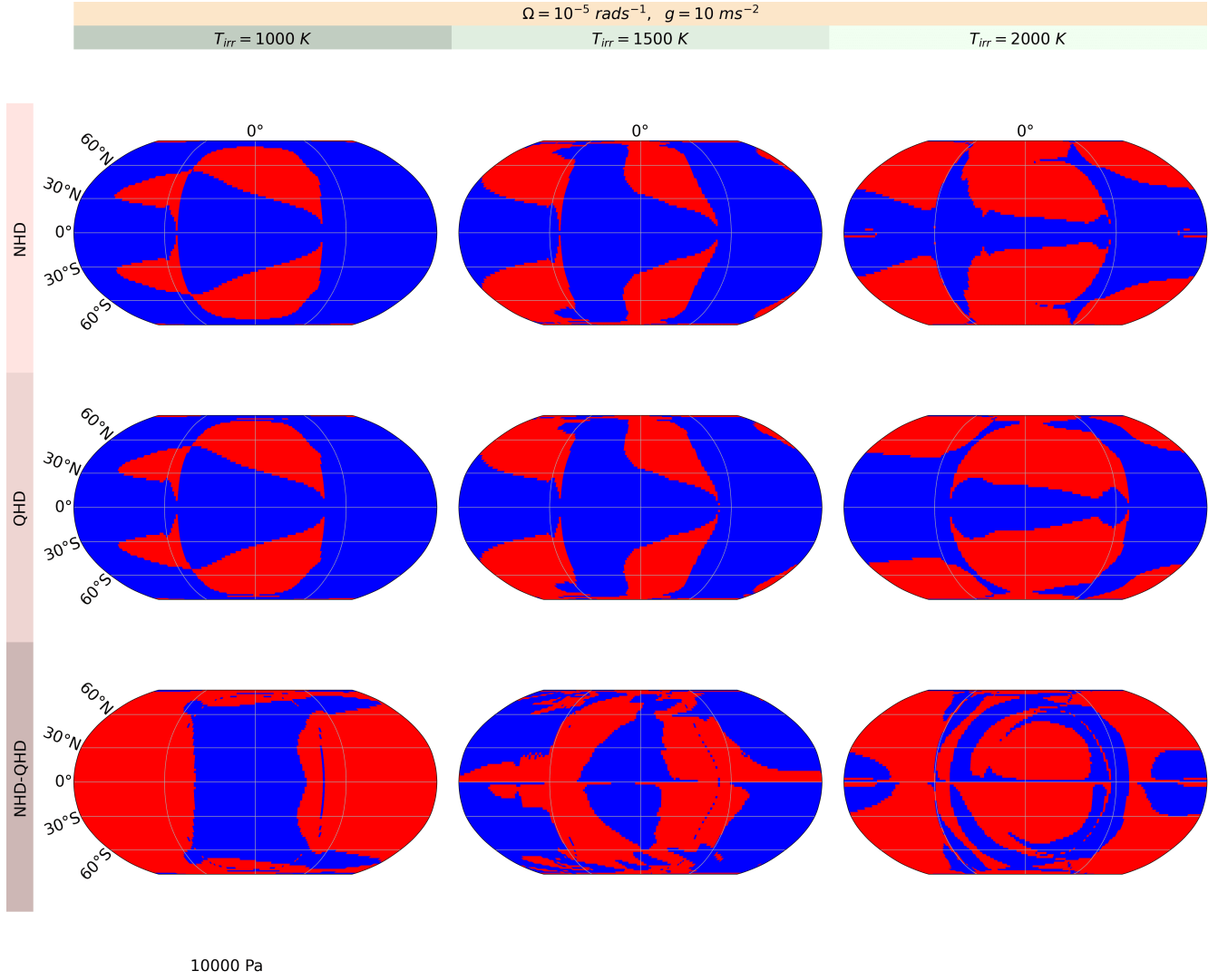


**Figure 35.** Sign of  $\frac{v \tan(\Phi)}{10w} - 1$  for the NHD and QHD equation sets with  $g = 10 \text{ ms}^{-2}$ ,  $\Omega = 1 \cdot 10^{-5} \text{ rad/s}$  and with altering  $T_{irr}$ . Blue and red regions show negative and positive values

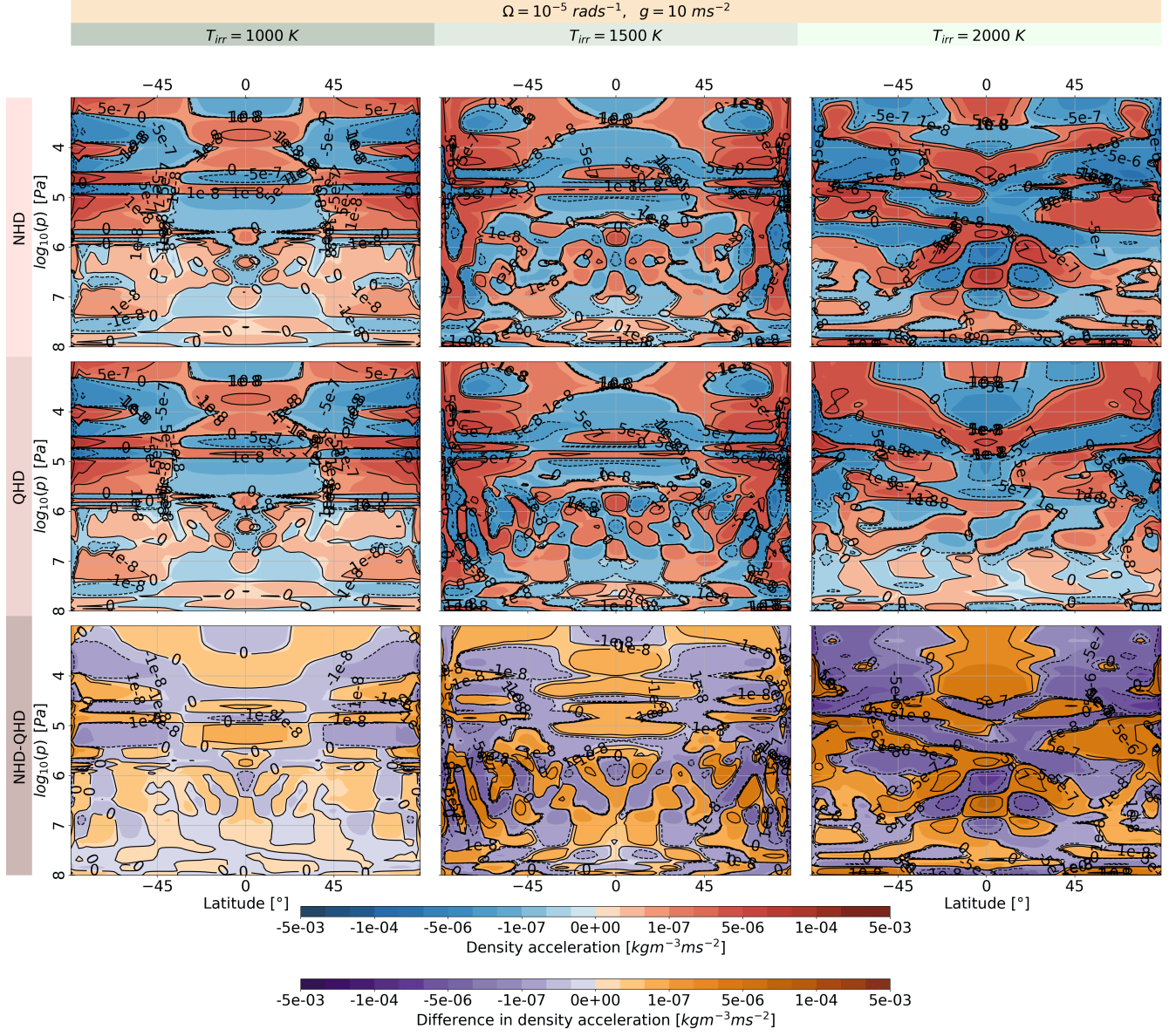


**Figure 36.** Horizontal acceleration for the NHD and QHD equation sets with  $\Omega = 1 \cdot 10^{-5} \text{ rad/s}$ ,  $g = 10 \text{ ms}^{-2}$  and with altering  $T_{irr}$ .

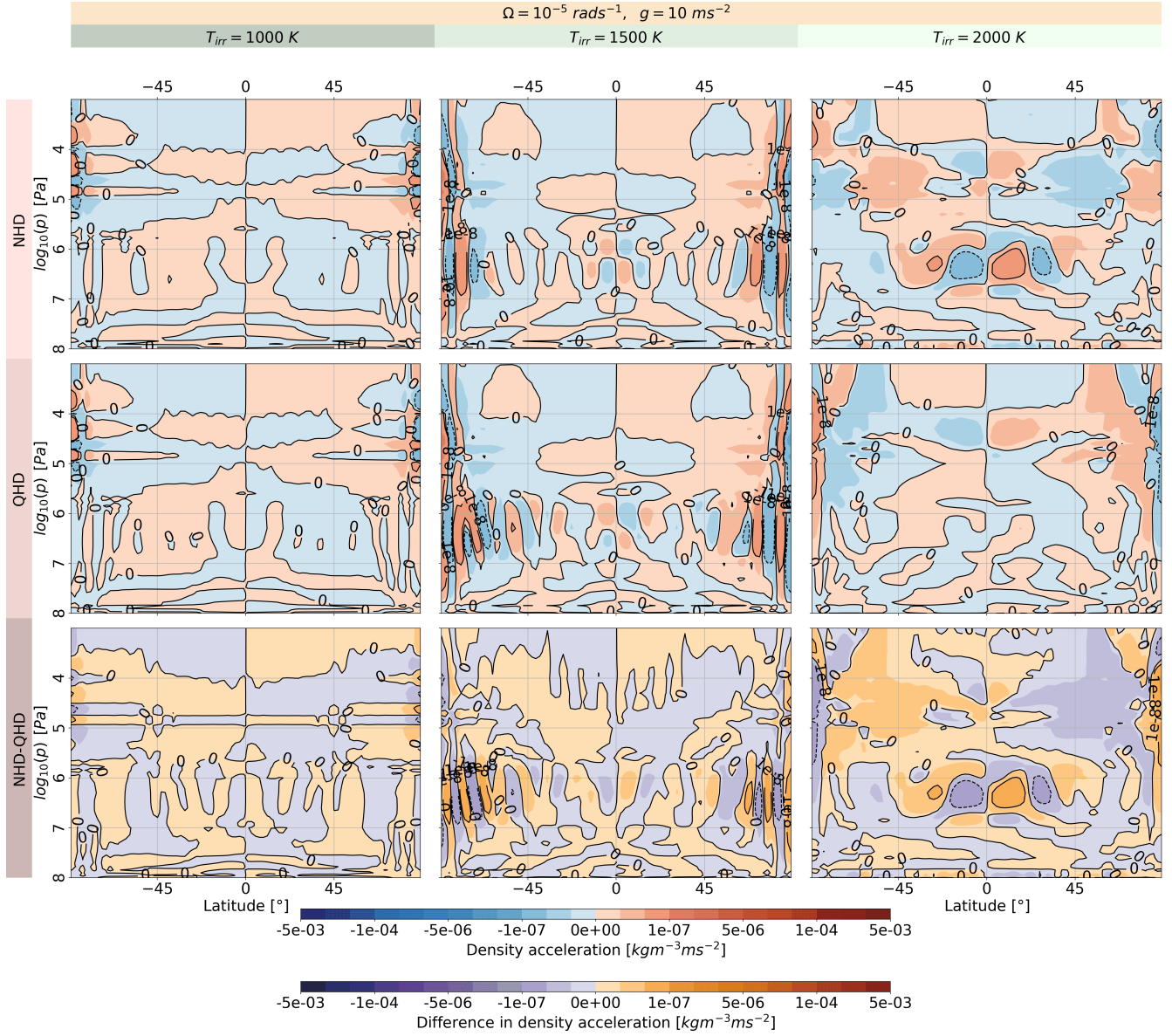


**Figure 37.** Vertical acceleration for the NHD and QHD equation sets with  $\Omega = 1 \cdot 10^{-5} \text{ rad/s}$ ,  $g = 10 \text{ ms}^{-2}$  and with altering  $T_{irr}$ .



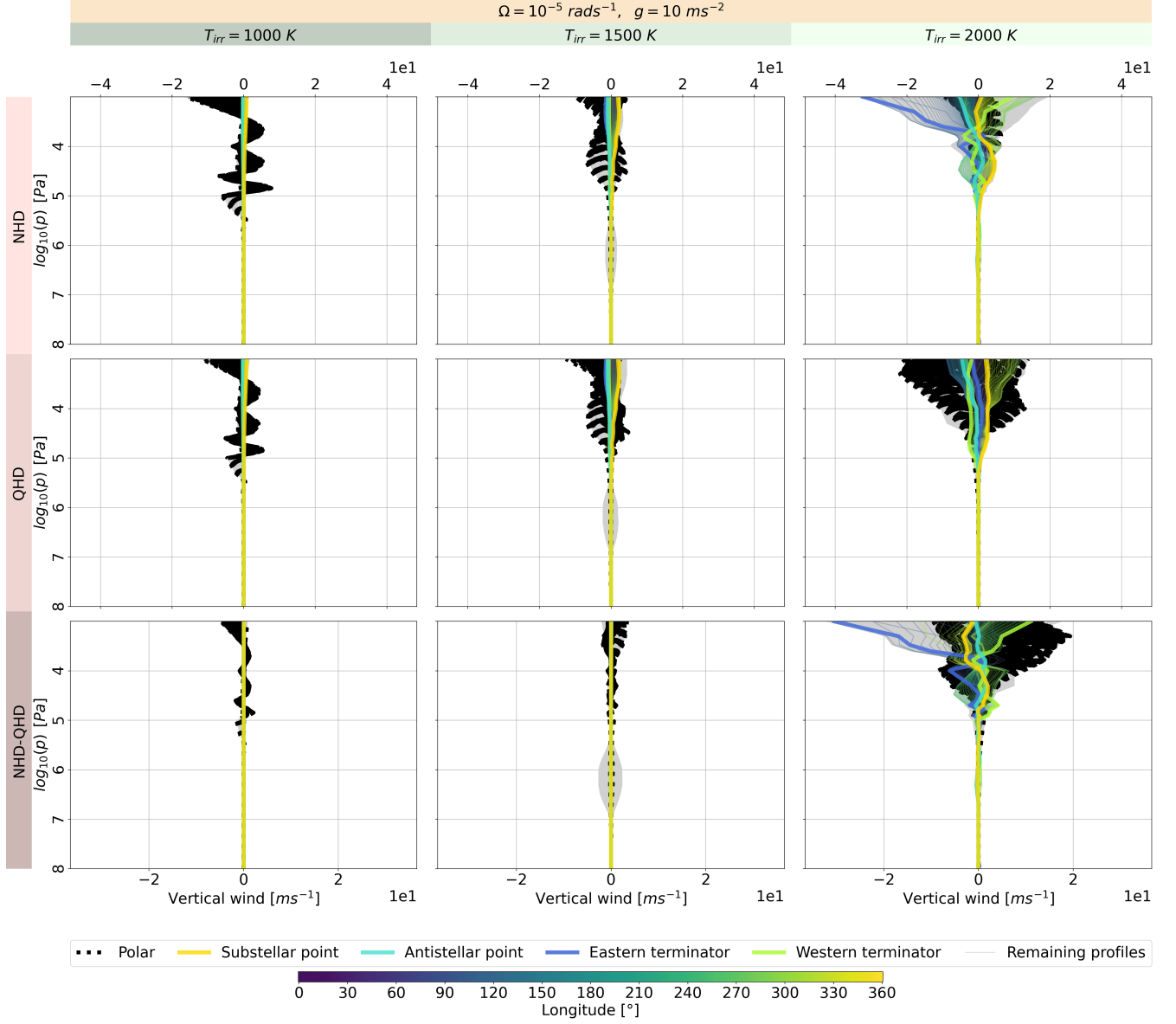


**Figure 38.** Vertical wind speed at each grid point for the NHD and QHD equation sets with  $g = 10 \text{ ms}^{-2}$ ,  $\Omega = 1 \cdot 10^{-5} \text{ rad/s}$  and with altering  $T_{irr}$ . The coloured lines indicate momenta profiles along the equator and its coordinates by the colourbar. The dotted black thin line shows momenta profiles at the latitudes 87°N and 87°S. The bold coloured lines represent momenta profiles at the western, eastern terminators, sub- and antistellar point. The grey lines represents all the other momenta profiles.

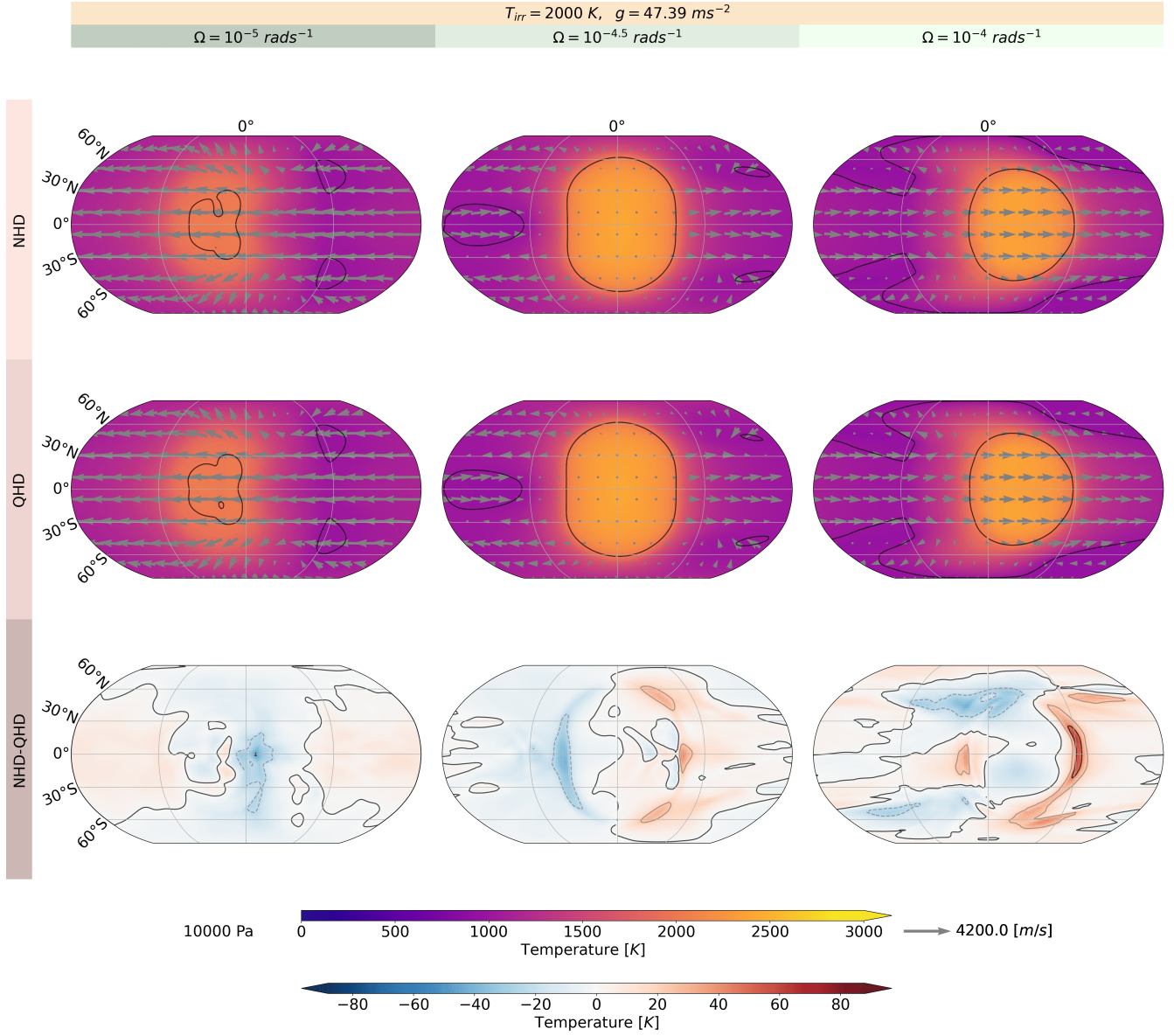


**Figure 39.** Temperature and wind speed at 10'000 Pa for the the NHD and QHD equation sets with  $g = 47.39 \text{ ms}^{-2}$ ,  $T_{irr} = 2'000 \text{ K}$  and with altering  $\Omega$ .

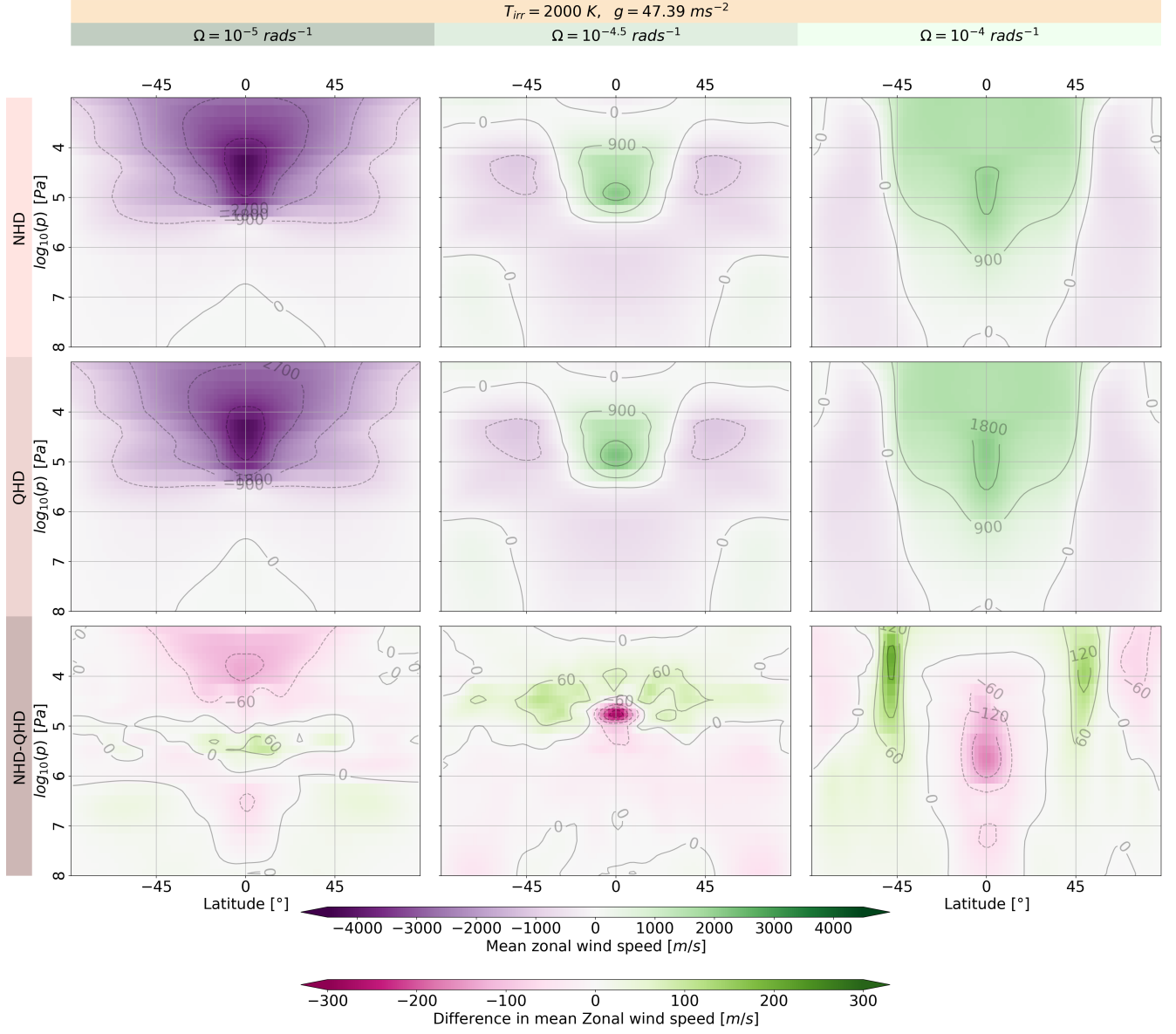


**Figure 40.** Zonal mean wind at each grid point for the NHD and QHD equation sets with  $g = 47.39 \text{ ms}^{-2}$ ,  $T_{irr} = 2'000 \text{ K}$  and with altering  $\Omega$ .

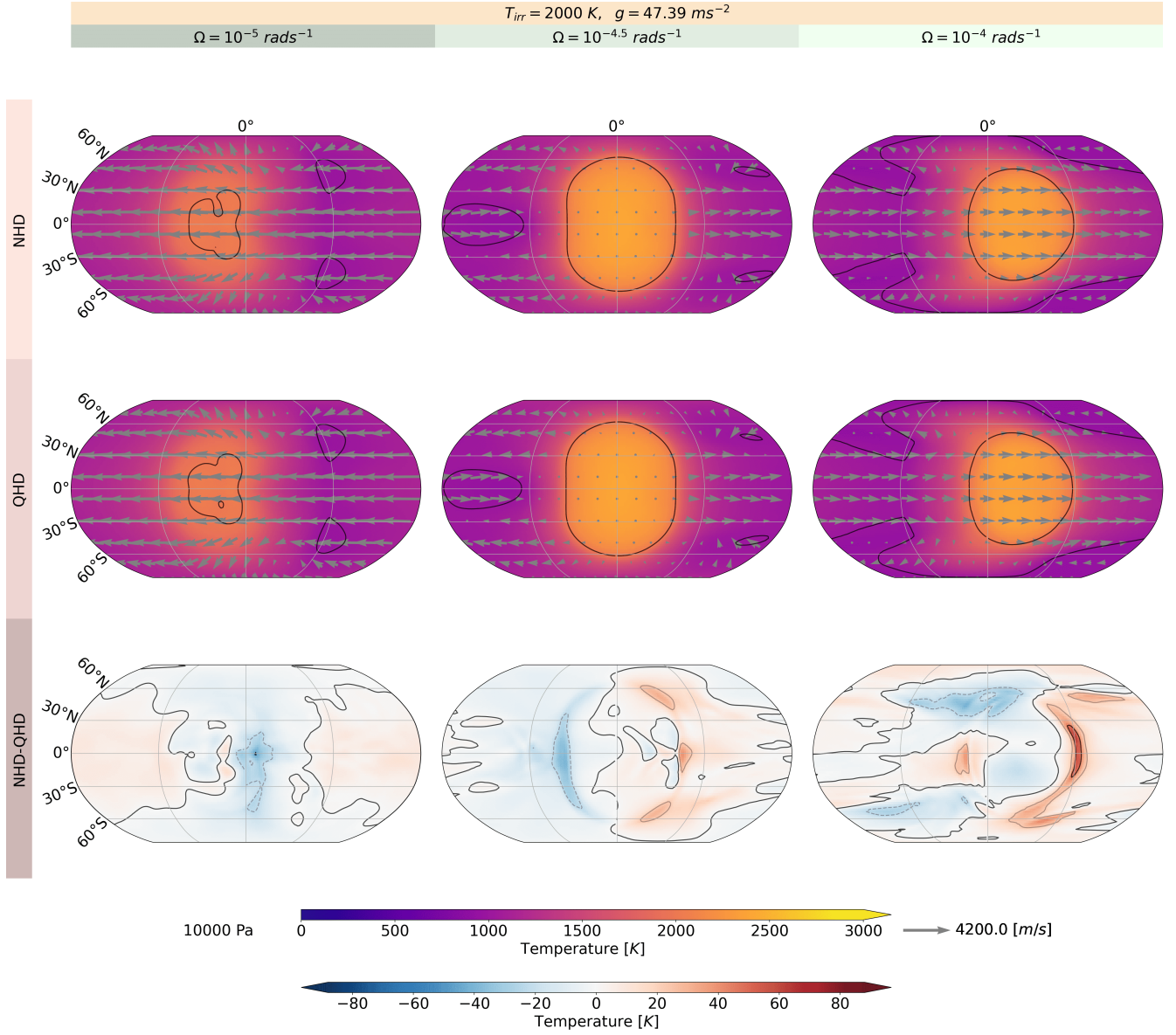


**Figure 41.** Temperature and wind speed at 10'000 Pa for the the NHD and QHD equation sets with  $g = 47.39$  ms $^{-2}$ ,  $\Omega = 1 \cdot 10^{-5}$  rad/s and with altering  $T_{irr}$ .



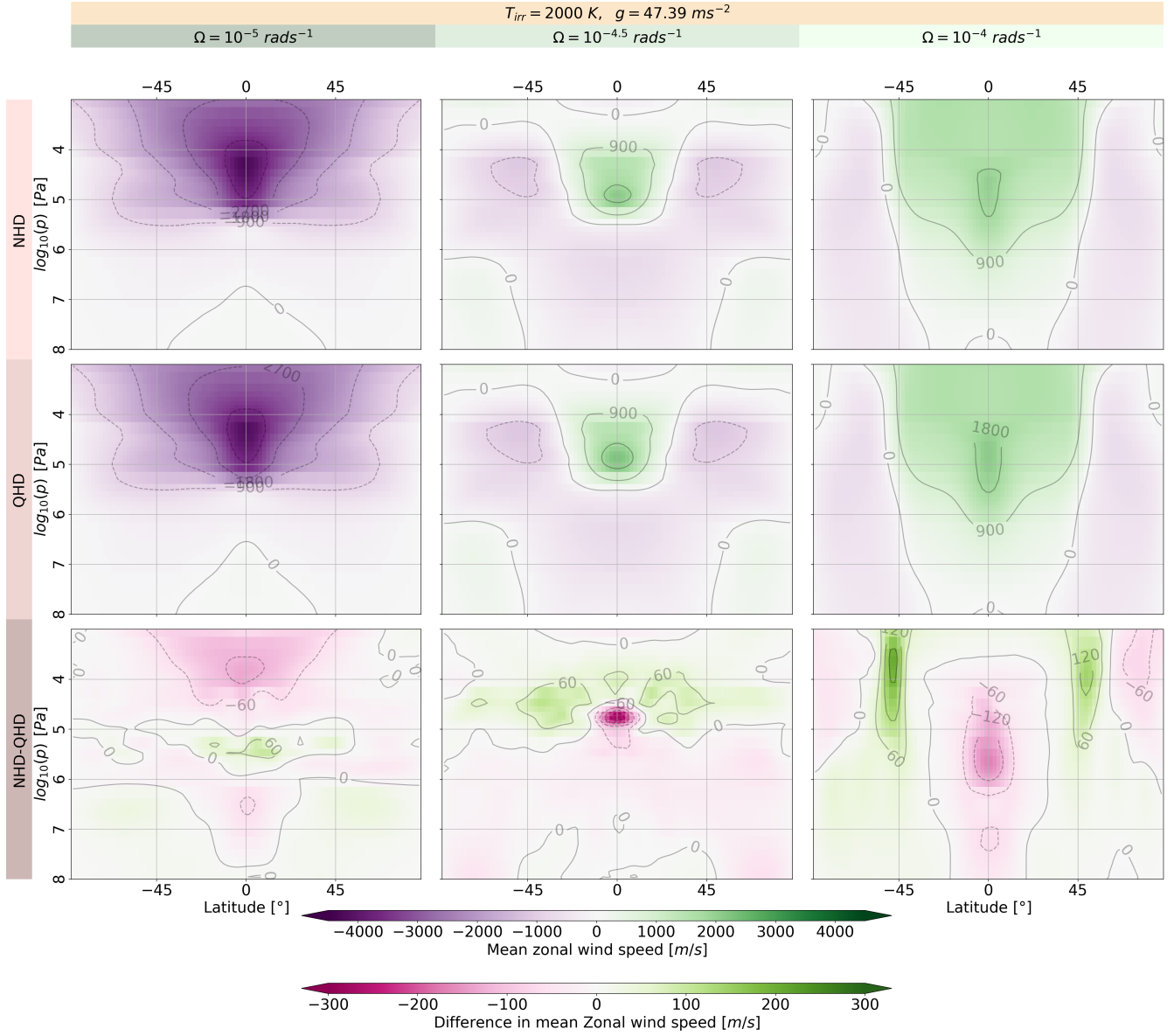


**Figure 42.** Zonal mean wind at each grid point for the NHD and QHD equation sets with  $g = 47.39 \text{ ms}^{-2}$ ,  $\Omega = 1 \cdot 10^{-5} \text{ rad/s}$  and with altering  $T_{\text{irr}}$ .